

Embedding Learning on Multiplex Networks for Link Prediction

Orell Trautmann^{1*}, Olaf Wolkenhauer^{1,2,3} and Clémence Réda⁴

¹Institute of Computer Science, University of Rostock, Rostock, 18057, Germany.

²Leibniz-Institute for Food Systems Biology at Technical University Munich, Freising, 85354, Germany.

³Stellenbosch Institute of Advanced Study, Wallenberg Research Centre, Stellenbosch, 7602, South Africa.

⁴BioComp, Institut de biologie de l'Ecole normale supérieure (IBENS), Ecole normale supérieure, CNRS, INSERM, PSL Université, Paris, 75005, France.

*Corresponding author(s). E-mail(s): orell.trautmann@uni-rostock.de;
Contributing authors: olaf.wolkenhauer@uni-rostock.de;
reda@bio.ens.psl.eu;

Abstract

Over the past years, embedding learning on networks has shown tremendous results in link prediction tasks for complex systems, with a wide range of real-life applications. Learning a representation for each node in a knowledge graph allows us to capture topological and semantic information, which can be processed in downstream analyses later. In the link prediction task, high-dimensional network information is encoded into low-dimensional vectors, which are then fed to a predictor to infer new connections between nodes in the network. As the network complexity (that is, the numbers of connections and types of interactions) grows, embedding learning turns out increasingly challenging. This review covers published models on embedding learning on multiplex networks for link prediction. First, we propose refined taxonomies to classify and compare models, depending on the type of embeddings and embedding techniques. Second, we review and address the problem of reproducible and fair evaluation of embedding learning on multiplex networks for the link prediction task. Finally, we tackle evaluation

on directed multiplex networks by proposing a novel and fair testing procedure. This review constitutes a crucial step towards the development of more performant and tractable embedding learning approaches for multiplex networks and their fair evaluation for the link prediction task. We also suggest guidelines on the evaluation of models, and provide an informed perspective on the challenges and tools currently available to address downstream analyses applied to multiplex networks.

Keywords: Multiplex Network, Node Embedding Learning, Network Representation Learning, Link Prediction, Knowledge Graph

1 Introduction

Networks have become a standard tool for modelling complex systems, due to their ability to abstract interactions between entities (Yang et al. 2023), and compile information into knowledge graphs. Networks (or graphs) are a diagrammatic representation of complex systems, which depict entities as nodes (or vertices) and their interrelations as edges (Estrada 2011). While classical network approaches have achieved tremendous success in modelling real-world problems (Kivelä et al. 2014), they do not adequately represent the variety of information. As such, over the past two decades, multiplex networks have grown in popularity (Kivelä et al. 2014; Boccaletti et al. 2014; Bianconi 2018). Multiplex networks are a collection of networks that share the same nodes but have different edge combinations, thereby representing a generalization of graphs. Multiplex networks are especially useful for representing interactions or connections between different entities from various perspectives, which is why they are sometimes also referred to as multi-view networks (Qu et al. 2017).

Multiplex networks have numerous real-life applications; for example, they can represent user interactions across social media platforms (Nguyen et al. 2015; Achour and Romdhane 2025) or protein-protein interactions across tissues (Zitnik and Leskovec 2017). More specifically, in the example on social media, multiplex networks can be used to model cross-platform social relationships. Such a network would consist of

multiple layers, each corresponding to an online social network (Nguyen et al. 2015) on a singular platform (*e.g.*, Facebook, Instagram, etc.). The social networks themselves are constructed in a way that the nodes correspond to people (their accounts) and the edges between them correspond to a friendship (or the action of following a user). Since people may have accounts across different social media platforms, these networks are interconnected, forming a network of networks (Boccaletti et al. 2014; Kivelä et al. 2014; Bianconi 2018). Similarly, in the example of tissue-specific protein-protein interactomes, the nodes correspond to proteins, and the edges represent their pairwise interactions, which may differ across the tissues considered, *i.e.*, , the layers. This multiplex network, therefore, characterizes the proteins’ tissue-dependent behaviors.

These networks are not only useful as a way to summarize data, they also play a crucial role in many machine learning and data mining tasks (El Gheche and Frossard 2021). Networks are intrinsically combinatorial objects without a vector space (Baptista et al. 2023). Network embeddings map these objects to a convenient latent space, which allows us to transform the information contained within into a machine learning-suitable representation. This process is also known as representation learning (Baptista et al. 2023), by essentially vectorizing nodes (Hajiseyedjavadi et al. 2019). As the use of multiplex networks in describing real-world systems has increased, efforts to generalize graph embeddings in the multiplex context have also grown. The difficulty here lies in producing vector representations for each node utilizing the additional information from other network layers. The vectorized forms of the networks are then used in downstream tasks such as node classification (Sun et al. 2019), community detection (Wilson et al. 2021), network reconstruction (Zhang and Kou 2022), and link prediction (Wang et al. 2023).

In link prediction, the goal is to infer the presence or the absence of a connection between two nodes (Lichtnwalter and Chawla 2012; Sharma and Singh 2016). For the

cross-platform example, this could be understood as suggesting new friends on Facebook, given the friendship information from all social media platforms. Similarly, link prediction allows us to uncover novel protein-protein interactions in protein-protein interactomes. The challenge is that the prediction relies on the view, or the layer of connections, so the embeddings must also capture both the differences and similarities across views or layers of the multiplex network.

Many models have been proposed for embedding learning on networks for link prediction (Liu et al. 2017; Zitnik and Leskovec 2017; Zhang et al. 2018; Zhang and Kou 2022; Gallo et al. 2024). Yet, to our knowledge, apart from a very brief review on multiplex network embeddings for clustering (Han et al. 2021), there has been no substantial review of multiplex network embedding methods. Furthermore, the various types of latent representation vectors used in the literature have not yet been classified.

Our contributions to the field are as follows: first and foremost, in Section 3.1 we introduce a first representation or embedding taxonomy for multiplex network embeddings. Second, in Section 3.2, we extend and refine an existing classification of embedding techniques on single-layer network embeddings (Baptista et al. 2023) to multiplex networks, incorporating an additional aggregation category (Liu et al. 2017). Then, this method taxonomy is leveraged to provide a detailed, yet general, description of the pros and cons of each type of embedding technique. In particular, we will focus on approaches that permit the integration of information from different views of the multiplex networks. Third, we discuss and propose guidelines for the evaluation problem on link prediction in Section 4. Moreover, we aim to address the evaluation on directed multiplex networks by introducing a new testing procedure.

2 Definitions and Preliminaries on Networks

Here, we introduce the relevant terminology and notation for the next sections. For a detailed description of multiplex networks, the reader is referred to Boccaletti et al.

(2014); Kivelä et al. (2014); Bianconi (2018). We begin with a brief overview of the relevant terminology and notation for “simple” graphs, which we will use recurrently throughout this review.

A graph G is described by an ordered pair (V, E) , where $V := \{v_1, v_2, \dots, v_N\}$ is the set of nodes (or vertexes), $E \subseteq V \times V$ is the set of edges between pairs of nodes. We distinguish between directed and undirected graphs. For undirected graphs, the pair $(v_1, v_2) \in E$ is unordered. In case of directed graphs, these pairs are indeed ordered, which means for $(v_1, v_2) \in E$, (v_2, v_1) need not necessarily be an element of E . The edges may additionally be weighted by the function $w : V \times V \rightarrow \mathbb{R}_+$. An unweighted graph can be understood as a weighted network with values in $\{0, 1\}$. Finally, the information from the graph can be represented by the adjacency matrix $\mathbf{A} = (w(v, u))_{(v, u) \in V \times V}$. The degree of a node v is the sum of the weights of the edges connected to it, *i.e.*, $\deg(v) = \sum_{u \in V} w(u, v)$. The degree matrix of the network is the diagonal matrix $\mathbf{D} = \text{diag}(\deg(v_1), \dots, \deg(v_N))$. These matrices play an important role in neural network-based methods that we will cover in Section 3.2.5.

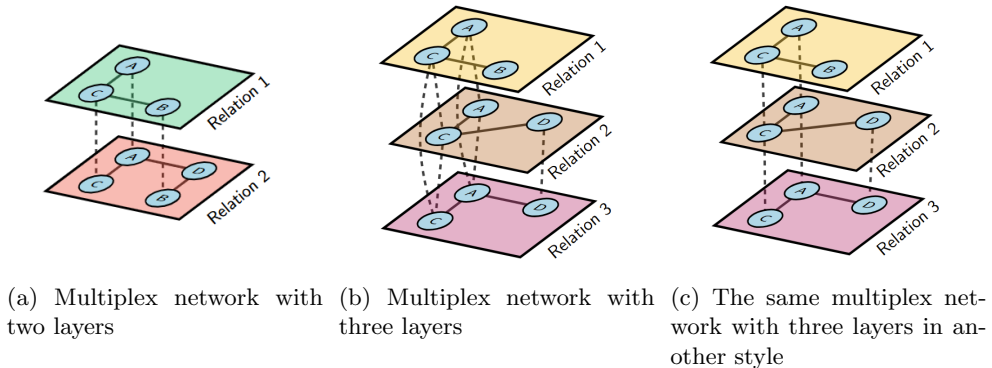


Figure 1: Examples of multiplex networks. Each layer corresponds to a specific relation, or view, in the network. The dashed lines represent interlayer connections between replica nodes (same entity represented on different layers), which are the only allowed type of interlayer edges in multiplex networks, whereas solid lines match intralayer connections. Figures 1b and 1c both show the same network using two different styles: with an edge to every replica node or simply edges to connect the layers from the top layer to the bottom layer.

In prior works, many authors use the terms “single-layer network” or “monoplex network” to make a clear distinction between networks featuring a single view, and those with several views or layers (De Domenico et al. 2013; Boccaletti et al. 2014; Kivelä et al. 2014) (Figure 1). Two mathematical notations for multiplex networks seem to prevail in the literature. The notation from Bianconi (2018) and Boccaletti et al. (2014) emerged from the realm of physics, whereas Kivelä et al. (2014) introduces notation more closely related to the literature in computer science. As it is more common in the methods we have reviewed, we will rely on the notation in Bianconi (2018) and Boccaletti et al. (2014).

Definition 1 (Multiplex Network) A multiplex network is a pair $\mathcal{M} = (Y, \mathcal{G})$, where $Y = \{1, \dots, M\}$ is the set of layers, and $\mathcal{G} = \{G_\alpha\}_{\alpha=1}^M$ is a family of graphs $G_\alpha = (V_\alpha, E_\alpha)$ with $\bigcap_{\alpha \in Y} V_\alpha \neq \emptyset$. Graph G_α on layer α can be undirected, directed, and/or weighted.

Nodes representing the same entity in different layers are called replica nodes (Bianconi 2018). To distinguish between replica nodes, we will use the notation $v_i^{[\alpha]}$ for entity $v_i \in V$ on layer $\alpha \in Y$. Edges within a layer, *i.e.*, the elements of $(E_\alpha)_\alpha$, are called intralayer edges. On the other hand, only connections between replica nodes are allowed when considering edges crossing layers. Edges between replica nodes of different layers are referred to as interlayer edges. We say the multiplex is node-aligned if $V_\alpha = V$ for all $\alpha \in Y$ (Kivelä et al. 2014). As depicted in Figure 1, it may be the case that nodes in some of the layers are missing. Without a loss of generality, one can assume that all layers feature the same set of nodes V , except that some of the nodes will be isolated depending on the layer (Kivelä et al. 2014).

Similarly to graphs, multiplex networks can be represented by their supra-adjacency matrix \mathbf{A} .¹ For the family of adjacency matrices $\{\mathbf{A}_\alpha\}_{\alpha=1}^M$ corresponding to \mathcal{G} , and if $N = \#V$ be the number of distinct nodes, then the corresponding

¹Usually, the supra-adjacency matrix is introduced as the flattened adjacency tensor of \mathcal{M} (Kivelä et al. 2014; Boccaletti et al. 2014; Bianconi 2018). This explanation is omitted as it is not used in our review.

supra-adjacency matrix is given by

$$\mathcal{A} = \begin{pmatrix} \mathbf{A}_1 & \mathbf{I}_N & \dots & \mathbf{I}_N \\ \mathbf{I}_N & \mathbf{A}_2 & \ddots & \vdots \\ \vdots & \ddots & \ddots & \mathbf{I}_N \\ \mathbf{I}_N & \dots & \mathbf{I}_N & \mathbf{A}_M \end{pmatrix}, \quad (1)$$

where \mathbf{I}_N is the identity matrix of dimension $N \times N$, with zeroes everywhere but on the diagonal, where all coefficients are set to 1. This structure will reappear in Section 3.2.3, which discusses random walk-based methods. With this notation in mind, we can now introduce embedding representation and method taxonomies.

3 Representation and Method Taxonomies

Taxonomies are essential for classifying models, leading to improved understanding and comparisons between methods. To our knowledge, the only other review on embedding techniques for multiplex networks is [Han et al. \(2021\)](#), and focuses on downstream clustering tasks. The authors differentiate between embedding approaches on single-layer networks, which are applied to each layer individually and then merge embeddings across layers to obtain a single embedding vector per node, and embedding learning on multiplex networks. However, they did not dwell further on the differences between methods. [Bielak and Kajdanowicz \(2024\)](#) gave a more detailed report on graph neural networks for representation learning on multiplex networks by introducing a taxonomy on information fusion for graph neural networks (GNN). Nevertheless, this taxonomy cannot be straightforwardly extended to multiplex network embeddings. Therefore, we provide a general taxonomy for multiplex network embedding methods.

Additionally, we establish that the latent representation embedding vectors obtained in multiplex networks are more nuanced than in monoplex networks. The

different types of representation vectors are sometimes mentioned in papers (Chen et al. 2024; Qu et al. 2017), yet have not been discussed so far. As such, we also introduce a representation taxonomy to categorize the different kinds of representations, allowing for a deeper comparison between embedding models.

3.1 Representation Taxonomy

The task of network representation (or embedding) learning is to map the network information onto lower-dimensional latent variables $\mathbf{z} \in \mathbb{R}^d$, where $d \ll N$ (Sun et al. 2019; Hou et al. 2020). Similarly, the space \mathbb{R}^d is called the latent space or embedding space (Cui et al. 2019; Baptista et al. 2023). Prior works consider graph, edge and node embeddings. Here, we will focus only on node embeddings, which are the most commonly used (Baptista et al. 2023).

The embedding model is a mapping $f : V \rightarrow \mathbb{R}^d$, so that $f(v_i) = \mathbf{z}_i$ for all $v_i \in V$, where \mathbf{z}_i is the representation corresponding to node v_i . Baptista et al. (2023) gave five criteria for an efficient embedding method for monoplex networks: **(i)** Adaptability: it should be applicable to a variety of different types of networks: (un)directed, (un)weighted, and so on; **(ii)** Scalability: the application to bigger networks should be computationally feasible; **(iii)** Topology awareness: it should capture structural differences in the network, for instance, due to strongly or weakly connected nodes; **(iv)** Low dimensionality: it should encode the information into a lower-dimensional space; and finally **(v)** Continuity: the embedding space should be continuous.

However, the extension of these five criteria to multiplex networks is not so straightforward. Node representations in multiplex networks need to incorporate information from the whole network, across layers (*collaboration*), and to preserve the information of each layer individually (*preservation*) (Shi et al. 2018). Types of representations can then be categorized into three distinct groups.

First, unique embedding, or one-space models (Shi et al. 2018), or joint representation learning (Chen et al. 2024) produce a single representation per node (Ning et al. 2018; Zhang and Kou 2022). This representation also holds for all replica nodes in other layers. Mathematically, we write that $f(v_i^{[\alpha]}; \mathcal{G}) = \mathbf{z}_i$ for all $v_i^{[\alpha]} \in V_\alpha$ and for all $\alpha \in Y$.

Second, in enriched embedding, or coordinated representation learning (Chen et al. 2024), each replica node has its own representation (Li et al. 2018; Zhang et al. 2018; Chen et al. 2024). Nevertheless, these representations include information from the other layers and, as such, are not merely a single-layer embedding. This can be formalized as follows: $f(v_i^{[\alpha]}; \mathcal{G}) = \mathbf{z}_i^{[\alpha]}$ for all $v_i^{[\alpha]} \in V_\alpha$ and for all $\alpha \in Y$.

Finally, for numerous embeddings, any node in any layer is associated with multiple embedding vectors according to its role in the network (Matsuno and Murata 2018), e.g., with a source and target node representation. Formally, this becomes $f(v_i^{[\alpha]}; \mathcal{G}) = \{\mathbf{z}_{i,1}^{[\alpha]}, \dots, \mathbf{z}_{i,k}^{[\alpha]}\}$, where k is the number of embeddings per node.

Some embedding models on multiplex networks also use so-called context embeddings (Shi et al. 2018; Song and Thiagarajan 2019). These were inspired by the word2vec model from Mikolov et al. (2013a), which represents words as contexts for other words within a sentence, and were later applied to embedding learning in networks (Perozzi et al. 2014). However, they do not fall into the scope of our review, as context embeddings are not used in the subsequent prediction tasks, but discarded after the embedding learning step. These types of embeddings are found in various models, including random walk and optimization-based models, as described in Section 3.2.

Unique embeddings implement a strong collaboration (Shi et al. 2018), while single-layer embeddings are reflective of preservation without collaboration. Enriched embeddings might achieve a combination of collaboration and preservation. This spectrum is represented in Figure 2. On the one hand, unique embeddings may not

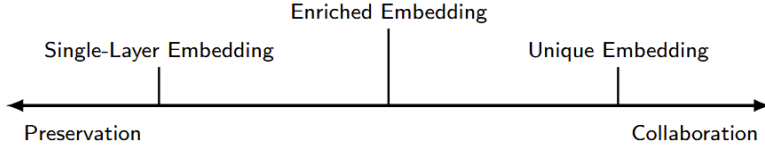


Figure 2: Single-layer embeddings, enriched embeddings, and unique embeddings fall onto the same spectrum of preservation and collaboration (Shi et al. 2018).

preserve enough layer-specific information to perform well on the task of layer-specific link prediction. As an example, without loss of generality, consider the binary predictor $\mu : \mathbb{R}^d \times \mathbb{R}^d \rightarrow \{0, 1\}$ that indicates the absence or the presence of an edge given the embeddings of the corresponding nodes. Then, resorting to our notation, $\mu(f(v_i^{[\alpha]}; \mathcal{G}), f(v_j^{[\alpha]}; \mathcal{G})) = \mu(\mathbf{z}_i, \mathbf{z}_j)$. This means that such a predictor on unique embeddings would add or subtract the edge to every layer in the network. On the other hand, enriched embeddings are designed to overcome this shortcoming. Furthermore, considering the widespread use of symmetric prediction methods (see Section 4.2), numerous embeddings—specifically target and source node representations—might considerably improve edge predictions for directed networks, as they reflect asymmetry. Moreover, numerous embeddings allow for better role-specific representations and thus increased topology awareness (criterion (iii)), though the number of embeddings directly impacts low-dimensionality (criterion (iv)).

All in all, the choice of embedding representation involves balancing the amount of preservation and collaboration required to tackle the downstream task, and should be carefully considered depending on the type of embedding techniques, which we review in the next section.

3.2 Method Taxonomy

Many taxonomies have been proposed for embedding techniques in monoplex networks, as evidenced by the number of available surveys (Cui et al. 2019; Hou et al. 2020;

Zhang et al. 2020; Baptista et al. 2023), though *not* in multiplex networks as in our review.

For instance, Hou et al. (2020) gives a two-level taxonomy. The first one splits methods into embeddings of dynamic and static monoplex networks. The second level classifies the static methods similarly to Cui et al. (2019) into embeddings with structural information, and embeddings with additional information (*e.g.*, , node attributes). Yet, as the scope of this paper is on multiplex networks without additional information, this taxonomy is not relevant in our case.

Zhang et al. (2020) make a distinction between unsupervised and supervised models for embedding learning in monoplex networks. While this classification makes sense, we believe the taxonomy introduced by Baptista et al. (2023) to be more adequate, as it categorizes models into groups of common mathematical approaches instead of learning paradigms. The naive extension of these groups to multiplex networks is straightforward, yet it would neglect a whole class of methods based on an aggregation approach across layers.

The aforementioned review on clustering (Han et al. 2021) mentions traditional clustering approaches on networks, which do not use embeddings, generalized to multiplex networks, based on two main procedures. The first one involves the transformation of the multiplex network into a single-layer network, followed by the application of a clustering method for monoplex networks. The second procedure consists in individually applying to each layer a clustering method for monoplex networks and then combining the results.

Bielak and Kajdanowicz (2024) introduce a taxonomy of methods for embedding learning named “fusion” restricted to graph neural networks (GNNs). Their taxonomy identifies four types of fusion: graph-level, GNN-level, embedding-level, and prediction-level fusions. However, it is important to note that both prediction-level and GNN-level fusion are not applicable to the context of network representation. Indeed, all

models inherently combine information, rendering GNN-level fusion unnecessary, while prediction-level fusion does not influence the embeddings.

We propose a method taxonomy with two levels, similarly to [Baptista et al. \(2023\)](#). We first make a high-level distinction between shallow and deep methods. In short, deep methods have hidden layers, shallow methods do not. As such, it is straightforward to see that neural network-based methods (*e.g.*, graph convolution neural networks, or GCNs) are deep methods, and all other methods are shallow methods. The second lower-level level of taxonomy considers random walk, optimization, matrix factorization, and aggregation-based methods, the latter being more isolated from all other former groups. Over the next few sections, we will describe the characteristics of each group. We illustrate the distinction between representation and method taxonomies in Table 1.

Table 1: Representation and method taxonomies on the literature on embedding learning in multiplex networks for link prediction. The rows correspond to the type of representation, whereas the columns are organized by the technique used in the embedding model.

Embedding Representation	Embedding Method					
	Matrix Factorization	Shallow		Deep		
		Random Walk	Optimization	Neural Networks	Aggregation	
Unique Embedding		RMNE		MGAT		
		MDeepWalk		MultiplexSAGE		
		FFME		DGMI		
		mpx2vec		mGCN		
		MultiVERSE		VANE		
		MANE+		MEGAN		
		MVN2VEC				
Enriched Embedding		MHME				
		Multi-node2vec				
		MANE	MNE	CGNN		
			NANE	LIAMNE		
Numerous Embedding			RWM	MUNEM	MNI	
			OhmNet			
				MELL		

3.2.1 Aggregation Methods

As the name suggests, the aggregation, also called fusion (Bielak and Kajdanowicz 2024), method merges or fuses information together in the multiplex network. We can distinguish between a network-level and an embedding-level information aggregation. The latter is sometimes referred to as *results aggregation* (Liu et al. 2017). A visual depiction of both aggregation approaches is given in Figure 3.

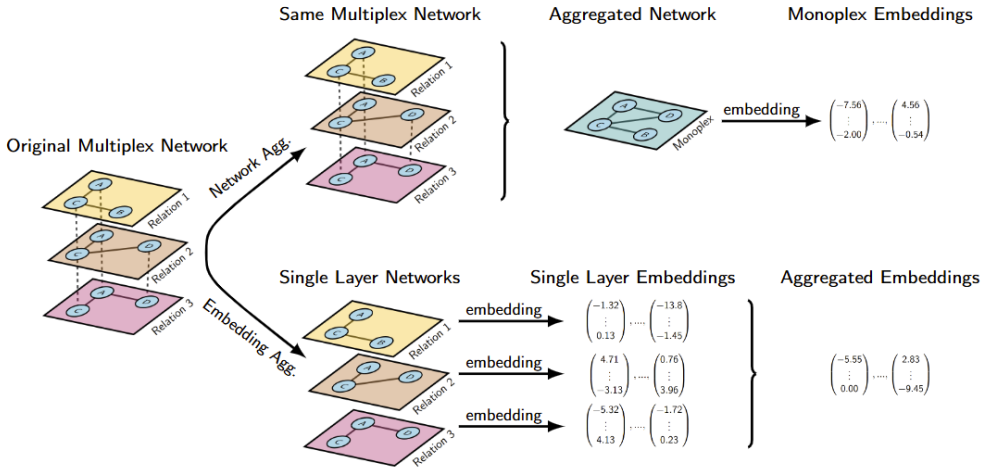


Figure 3: Difference between network-level and embedding-level aggregations. The aggregation step is depicted by the braces.

First, in network aggregation, the information of the multiplex network is fused down to produce a simple network onto which the embedding method is then applied. In other words, the goal is to construct a graph $\tilde{G} = (V, \tilde{E})$ from \mathcal{G} by some method Agg with $\tilde{\mathbf{A}} = \text{Agg}(\mathbf{A}_1, \dots, \mathbf{A}_M)$ the corresponding adjacency matrix for the aggregated network. The difficulty lies in fusing the multiplex into a single network, while retaining as much information on the diverse node relations as possible. Different types of network-level aggregation have been introduced (usually in the realm of complex system physics), for instance, average network, projected monoplex network, and overlay network (Sánchez-García et al. 2014). One of the PMNE model (Liu et al.

2017) variants combines the layers of the multiplex network into a weighted network by summing the edge weights; formally: $\text{Agg}(\mathbf{A}_1, \dots, \mathbf{A}_M) = \sum_{\alpha \in Y} \mathbf{A}_\alpha$.

In any case, aggregating the layers into a single network implies information loss, as it somewhat neglects the preservation objective from Section 3.1. This information loss was quantified and leveraged by De Domenico et al. (2015) to minimize loss during aggregation.

On the other hand, the embedding-level aggregation first applies an embedding method for monoplex networks on each layer to obtain one representation for each replica node, and then aggregates the representations of an entity across layers to produce a single representation for all replica nodes of a single entity. More formally, the goal is to construct a latent vector $\tilde{\mathbf{z}}_i \in \mathbb{R}^d$ to node $v_i \in V$ from embeddings $\mathbf{z}_i^{[1]}, \dots, \mathbf{z}_i^{[M]}$ associated with replica nodes $v_i^{[1]}, \dots, v_i^{[M]}$ by some method Agg , with $\tilde{\mathbf{z}}_i = \text{Agg}(\mathbf{z}_i^{[1]}, \dots, \mathbf{z}_i^{[M]})$. An example of an aggregation function would be the mean across layers of replica representations, as done for a baseline method in Pio-Lopez et al. (2021). Another variant of the PMNE model (Liu et al. 2017) directly concatenates the layer-specific representations, that is, $\text{Agg}(\mathbf{z}_i^{[1]}, \dots, \mathbf{z}_i^{[M]}) = \text{concat}_{\alpha \in Y} \mathbf{z}_i^{[\alpha]} \in \mathbb{R}^{Md}$. A more sophisticated approach in the MNI model (Wang et al. 2023) aggregates the embeddings for each layer by maximizing the mutual information between the latent vectors. Depending on the approach, embedding-level fusion can allow for some collaboration, whilst preserving more layer-specific information.

Liu et al. (2017) and Bielak and Kajdanowicz (2024) compared the performance of models when using network-level aggregation, embedding-level aggregation, and a version not based on aggregation, allowing for more collaboration. They concluded that the aggregation methods performed the worst for link prediction. This might explain why, while aggregation is a straightforward option, it is rarely used. Some models still use embedding-level aggregation after having implemented a collaborative model to

retrieve unique embeddings (Shi et al. 2018; Ata et al. 2021), though it is rare. However, aggregation is still prominently used with monoplex-network-specific embedding methods as baseline methods (Liu et al. 2017). Indeed, embedding models for multiplex networks are often compared to LINE (Tang et al. 2015), DeepWalk (Perozzi et al. 2014), or struc2vec (Ribeiro et al. 2017) combined with either network-level (Sun et al. 2019; Ning et al. 2021b; Chen et al. 2024) or embedding-level (Hajiseyedjavadi et al. 2019; Pio-Lopez et al. 2021) fusion.

3.2.2 Matrix Factorization

Matrix factorization models take advantage of the fact that the (potentially weighted) adjacency matrix \mathbf{A} holds all the information about the graph (Baptista et al. 2023). Therefore, these methods apply classical matrix factorization techniques from linear algebra to obtain representation vectors. In particular, those methods often rely on the definition of the Laplacian \mathbf{L} of a network, defined by the difference of the degree and the adjacency matrices of the network, *i.e.*, $\mathbf{L} = \mathbf{D} - \mathbf{A}$, where the degree matrix \mathbf{D} is a diagonal matrix containing the degree of each of the N nodes. Moreover, we also define the normalized Laplacian matrix $\widehat{\mathbf{L}} = \mathbf{D}^{-1/2} \mathbf{L} \mathbf{D}^{-1/2}$.

A comprehensive list of matrix factorization approaches developed for monoplex networks can be found in Baptista et al. (2023). A notable example is the Laplacian Eigenmaps (Belkin and Niyogi 2001), where embedding vectors preserve the closeness of the nodes in the network with respect to their edge weights. Laplacian Eigenmaps are obtained by maximizing a trace involving the Laplacian of the network and the matrix of concatenated embedding vectors $\mathbf{Z} \in \mathbb{R}^{N \times d}$: $\max_{\mathbf{Z}} \text{tr}(\mathbf{Z}^T \mathbf{L} \mathbf{Z})$, under the constraint $\mathbf{Z}^T \mathbf{D} \mathbf{Z} = \mathbf{I}_d$.² The constraint allows the authors to remove an arbitrary scaling factor in the embeddings.

²The trace $\text{tr}(M)$ of a matrix M takes the sum of the diagonal elements of the matrix.

In MANE (Li et al. 2018), this trace maximization approach is extended to the multiplex case by computing enriched embeddings. To this end, the authors split the objective into two components: (1) the intralayer objective, which is the straightforward extension of the monoplex formulation to each layer: $\max_{\mathbf{Z}_\alpha} \text{tr}(\mathbf{Z}_\alpha^\top \widehat{\mathbf{L}}_\alpha \mathbf{Z}_\alpha)$ under the constraint $\mathbf{Z}_\alpha^\top \mathbf{Z}_\alpha = \mathbf{I}$ for all layer $\alpha \in Y$; and (2) the interlayer objective, which is:

$$\min_{\mathbf{Z}_\alpha, \mathbf{Z}_\beta, \mathbf{K}_{\alpha\beta}} \sum_{\alpha, \beta=1}^M \|\mathbf{I}_N - \mathbf{Z}_\alpha^\top \mathbf{K}_{\alpha\beta} \mathbf{Z}_\beta\|_F^2, \text{ such that } \mathbf{Z}_\alpha^\top \mathbf{Z}_\alpha = \mathbf{I}_N, \text{ for all layers } \alpha \in Y,$$

where $\mathbf{K}_{\alpha\beta} \in \mathbb{R}^{n \times n}$ is the interlayer adjacency matrix between layers α and β . Together, these objectives are merged into the following trace maximization problem:

$$\max_{\mathbf{Z}_\alpha} \text{tr} \left(\mathbf{Z}_\alpha^\top \left(\widehat{\mathbf{L}}_\alpha + \lambda \sum_{\beta \in Y} \mathbf{Z}_\beta \mathbf{Z}_\beta^\top \right) \mathbf{Z}_\alpha \right), \text{ such that } \mathbf{Z}_\alpha^\top \mathbf{Z}_\alpha = \mathbf{I}_N, \forall \alpha \in Y.$$

The formulation above is the multiplex case of the more general multilayer network description in Li et al. (2018). MANE has so far been the only published work to use matrix factorization for generating node embeddings on multiplex networks. Nevertheless, random walk approaches, which will be discussed in the next section, appear to be closely related to matrix factorization, as some researchers have noticed (Qu et al. 2018).

3.2.3 Random Walk-Based Methods

A random walk on a graph is a sequence of points obtained by starting at an initial node, randomly selecting an edge to traverse to the next node, and then iterating this procedure (László et al. 1996). Typically, edges are selected with a probability proportional to the edge weight, which allows the random walker to explore the network

structure. The element $[\mathbf{P}]_{ij}$ of the transition matrix $\mathbf{P} = \mathbf{D}^{-1}\mathbf{A}$ gives the probability that a random walker will move from node v_i to v_j , for \mathbf{D} and \mathbf{A} respectively the degree and adjacency matrix of a monoplex network. Formally, we write this as $p(v_i, v_j) = [\mathbf{P}]_{ij} = w(v_i, v_j)/\deg(v_i)$. The position update from step n to step $n+1$ of the random walker is achieved by computing $\mathbf{m}_{n+1} = \mathbf{P}^\top \mathbf{m}_n$, where \mathbf{m}_n and \mathbf{m}_{n+1} are probability vectors in \mathbb{R}^N , where N is the number of nodes in the graph. This process, known as the standard random walk and its variants, is at the heart of this section. A visualization of the two most central random walk methods, random walk and random walk with restart—where the random walker is allowed to teleport back to the starting node (referred to as the *seed node* (Baptista et al. 2022))—is given in Figure 4.

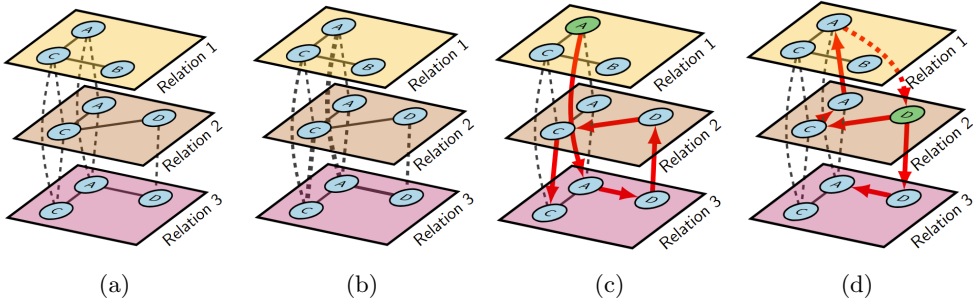


Figure 4: Figure 4a shows the original multiplex network. Figure 4b displays the transition probabilities for the random walk: the thicker the line, the higher the probability of walking this edge. Figure 4c depicts a random walk using the most likely node transitions, where the green node is the seed of the random walk, and the red arrows the path taken. Figure 4d illustrates a random walk *with restart* on a multiplex network, where the dashed red arrow indicates the teleportation back to the seed node.

Random walk-based methods for embedding learning on monoplex networks began with DeepWalk (Perozzi et al. 2014), which was inspired by the natural language processing model word2vec (Mikolov et al. 2013a). Since then, many researchers have worked on advancing the approach, introducing prominent variants such as node2vec (Grover and Leskovec 2016) or struct2vec (Ribeiro et al. 2017). node2vec (Grover and Leskovec 2016) adapted the DeepWalk model by using a biased

second-order random walk—meaning that the walker remembers the last step taken—and using the Skip-Gram objective (Mikolov et al. 2013a) combined with Alias table sampling (Li et al. 2014) for optimization. The Skip-Gram objective takes in a sampled sequence of nodes, and maximizes the likelihood for two nodes close to each other in the sequence. Formally, this is written as

$$\max \frac{1}{T} \sum_{i=1}^T \sum_{-c \leq j \leq c, j \neq i} \log p(v_{i+j} | v_i), \quad (2)$$

where T is the size of the node sequence $S := \{v_1, v_2, \dots, v_T\}$, $\{v_{i-c}, \dots, v_{i-1}, v_{i+1}, \dots, v_{i+c}\} \cap S$ is the context window for node v_i , and $c \in \mathbb{N}$ is a constant and a hyperparameter of the objective. The Alias table sampling method is the random walk adaptation (Grover and Leskovec 2016) used to sample the node sequences.

Another approach on monoplex networks, struc2vec (Ribeiro et al. 2017), focuses on retrieving structurally informed embeddings. To this end, the authors construct a weighted multiplex network, where the k -th layer represents k -step connections, with the first layer being the original network. A k -step connection exists between two nodes if and only if one can go from one node to the other by walking exactly along k edges in the network. Then, the random walker starts at a node in the first layer and traverses the multiplex, where it is motivated to travel upwards to capture only the most structurally similar nodes. The path through the multiplex represents the sequence of nodes fed into the Skip-Gram objective function. These methods form a group of random walk methods, which we call *random walk sampling* procedures, as the goal of the random walk is to sample a sequence of nodes that will be fed to an objective function.

Unlike Baptista et al. (2023), we also consider random walk variants in which embedding learning is performed on the probability states \mathbf{m}^* , for instance, in

VERSE (Tsitsulin et al. 2018). VERSE uses the random walk with restart process defined in step $n > 0$ by:

$$\mathbf{m}_{n+1} = (1 - r)\mathbf{P}^\top \mathbf{m}_n + r\mathbf{m}_0, \quad (3)$$

where $r \in (0, 1)$ is the probability that the random walker will be teleported back to the seed node at each step. In the case where $r = 0$, we retrieve the standard random walk. However, for $r = 1$, the random walker does not move from his initial position. The parameter r thereby determines how local the walk will be. This process converges to a steady state \mathbf{m}^* as $n \rightarrow \infty$ (Page et al. 1999). If \mathbf{m}_0 is a unit vector, with $[\mathbf{m}_0]_i = 1$ and the other elements being 0, then $[\mathbf{m}^*]_j$ can be understood as a probability value for the proximity of node v_j to the unique seed node v_i . VERSE leverages this to construct embeddings by minimizing the cross-entropy between the resulting probability values from the random walk with restart process, and an estimator. We refer to these methods as *random walk limiting* procedures.

Huang et al. (2021b) proposed a general structure for random walk embedding approaches on monoplex networks. Three major components were identified as common to all random walk-based methods: the random walk process; the similarity function; and finally, the embedding algorithm. While these components have only been applied to monoplex networks and random walk sampling procedures, we will demonstrate that this framework can be extended to random walk-based methods for multiplex networks, including random walk limiting procedures. We use these components to explain the similarities and differences between the models.

Random walk process.

Huang et al. (2021b) classify the random walk processes of monoplex models into three categories: standard random walk, biased random walk, and PageRank (Berkhin 2005). A biased random walk is a random walk with modified transition probabilities

to prioritize certain transitions over others. The PageRank method teleports the random walker to a new (not necessarily connected) node with some probability at each iteration. In the multiplex context, we found only models using the random walk with restart (also known as rooted PageRank) or biased random walk algorithms.

The biased random walk is a truncated random walk with a fixed number of steps and transition probabilities that are no longer proportional to the edge weights. This method is used for node sequence sampling, which makes it a random walk sampling procedure. The general formula for the transition probability of the walker going from node i in layer α to node j in layer β is given by Ning et al. (2018):

$$p(v_i^{[\alpha]}, v_j^{[\beta]}) = \begin{cases} g_s(v_i^{[\alpha]}, v_j^{[\beta]}) & \text{if } \alpha = \beta \\ g_d(v_i^{[\alpha]}, v_j^{[\beta]}) & \text{if } i = j \\ 0, & \text{else} \end{cases} \quad (4)$$

where g_s describes the intralayer transition rule and g_d describes the interlayer transition rule. Diverse interlayer transition rules exist to achieve collaboration.

For instance, RMNE (Zhang and Kou 2022) favors interlayer transitions according to the structural similarity of the nodes. The walker can travel to neighboring nodes and structurally similar nodes, such as those with similar centrality and outgoing degree. For the interlayer transition, NANE (Chu et al. 2019) emphasizes using structurally similar replica nodes to reduce the “noise” in the embeddings from layers that differ significantly from the layer under consideration (named the *target layer*). They achieve this by comparing the vectors of the weighted averages of k -step adjacency matrices through the cosine similarity. Another approach for interlayer transitions is used in MDeepWalk (Song and Thiagarajan 2019), which extends the monoplex DeepWalk method to a multiplex scenario, where g_d equals to the Jaccard coefficient (Jaccard

1901) on the intralayer neighbors of replica nodes $v_i^{[\alpha]}$ and $v_i^{[\beta]}$.

$$g_d(v_i^{[\alpha]}, v_i^{[\beta]}) = \frac{\#\left(\mathcal{N}(v_i^{[\alpha]}) \cap \mathcal{N}(v_i^{[\beta]})\right)}{\#\left(\mathcal{N}(v_i^{[\alpha]}) \cup \mathcal{N}(v_i^{[\beta]})\right)},$$

where $\mathcal{N}(v_i^{[\alpha]})$ and $\mathcal{N}(v_i^{[\beta]})$ are the intralayer neighborhoods of $v_i^{[\alpha]}$ on layer α and $v_i^{[\beta]}$ on layer β , respectively. As a result, the random walker is more likely to move to replica nodes with similar neighborhoods. Similarly, Multi-node2vec (Wilson et al. 2021) extends the node2vec model to the even more general multilayer networks (Kivelä et al. 2014), by sampling nodes in the network as in node2vec with a second-order biased random walk. Multiplex networks are a special case of multilayer networks where only interlayer connections between replica nodes are allowed.

A different approach is taken by mpx2vec (Ning et al. 2018), which constructs *a priori* a node importance matrix $\mathbf{J} \in \mathbb{R}^{N \times M}$, with rows summing up to 1, and allocates a weight to each replica node. This matrix is first randomly initialized and then updated through a PageRank-inspired algorithm until convergence. The transition probabilities are then proportional to the product of those weights and to the distance τ between replica nodes on the same layer α : $p(v_i^{[\alpha]}, v_j^{[\beta]}) = \tau(v_i^{[\alpha]}, v_j^{[\alpha]}) \cdot [\mathbf{J}]_{i\beta}$.

Ning et al. (2021b) criticize the inherent bias of the random walk towards highly connected nodes. To counteract this bias, the authors propose two models, FFME and MHME. The interlayer transition rules in both models depend on the neighbor's partition coefficient (NPC), which they defined as:

$$\text{NPC}(v_i) = \frac{2}{\#\tilde{Y}(\#\tilde{Y} - 1)} \sum_{\alpha < \beta \leq M} \frac{\#\left(\mathcal{N}(v_i^{[\alpha]}) \cap \mathcal{N}(v_i^{[\beta]})\right)}{\#\left(\mathcal{N}(v_i^{[\alpha]})\right)},$$

where \tilde{Y} is the set of layers α in which the node $v_i^{[\alpha]}$ is not isolated, *i.e.*, of total degree 0. The NPC is used to ensure that interlayer jumps are primarily made between replica

nodes with different neighborhoods. The specific models then construct a multiplex network random walk that is designed with either a Metropolis-Hastings strategy (leading to the MHME model), or forest fire sampling (Leskovec and Faloutsos 2006) method (FFME model). The Metropolis-Hastings strategy modifies the random walk process to ensure that the resulting steady state has a uniform distribution over the nodes, demonstrating that this method does not favor highly connected nodes. On the other hand, the forest fire sampling method is able to capture the modularity of the network. Their experiments show that, on the task of link prediction, the MHME model generally outperforms the FFME model.

Unlike the previous methods, some methods independently perform a random walk on each layer. For instance, Luo et al. (2023) propose two variants of their model RWM: one with a biased random walk, and the other with a truncated random walk with restart. As the walkers traverse their respective network layers, they also influence the walkers in the other layers according to how similar their local structures are. This influence is captured in a relevance matrix that is updated with each step. This is how they achieve the collaboration in the resulting embedding.

In contrast to the aforementioned models, RWM requires a precomputed interlayer transition rule. Other models also fall into this category, applying the random walk on each layer separately and achieving collaboration in the optimization stage of the algorithm. This class includes the models OhmNet (Zitnik and Leskovec 2017), MVN2Vec (Shi et al. 2018), MNE (Zhang et al. 2018), and MANE+ (Ata et al. 2021)–not to be confused with MANE (Li et al. 2018) from the matrix factorization section. All of these truncated models require the number of steps of the truncated random walk to be set beforehand; a typical choice is a length of 10 steps.

The MultiVERSE (Pio-Lopez et al. 2021) extends the VERSE algorithm on monoplex networks to multiplex networks by using a random walk with restart method and is, therefore, a random walk limiting procedure. MultiVERSE introduces interlayer

transition probabilities $(\lambda_\alpha)_{\alpha \in Y}$ as hyperparameters, with $\sum_{\alpha \in Y} \lambda_\alpha = 1$. At each node in layer α , the walker moves to a replica node in layer $\beta \neq \alpha$ with probability λ_β or travels to an intralayer neighboring node layer α with probability λ_α . In other words, the probability of walking from node i on layer α to node j on layer β is:

$$p(v_i^{[\alpha]}, v_j^{[\beta]}) = \begin{cases} \lambda_\alpha \cdot p^{[\alpha]}(v_i^{[\alpha]}, v_j^{[\alpha]}) & \text{if } \alpha = \beta, \\ \lambda_\beta & \text{if } i = j, \end{cases}$$

where $p^{[\alpha]}(v_i^{[\alpha]}, v_j^{[\alpha]}) = [\mathbf{D}_\alpha^{-1} \mathbf{A}_\alpha]_{ij}$ is the i -th row and j -th column of the transition matrix of layer α . For this model, the transition hyperparameters $(\lambda_\alpha)_\alpha$ must be specified beforehand. In their paper, they simply set $\lambda_\alpha = \delta$ and $\lambda_\beta = (1-\delta)/(M-1)$, which yields the following supra-transition transition matrix:

$$\mathcal{P} = \begin{pmatrix} \delta \mathbf{P}_1 & \frac{1-\delta}{M-1} \mathbf{I}_N & \dots & \frac{1-\delta}{M-1} \mathbf{I}_N \\ \frac{1-\delta}{M-1} \mathbf{I}_N & \delta \mathbf{P}_2 & \ddots & \vdots \\ \vdots & \ddots & \ddots & \frac{1-\delta}{M-1} \mathbf{I}_N \\ \frac{1-\delta}{M-1} \mathbf{I}_N & \dots & \frac{1-\delta}{M-1} \mathbf{I}_N & \delta \mathbf{P}_M \end{pmatrix}.$$

Similarity function.

The node similarity function $\varphi : V \times V \rightarrow [0, 1]$ measures the topological similarity between pairs of nodes (Huang et al. 2021b). A value closer to 1 indicates a higher similarity between the two nodes, while a value closer to 0 suggests lower similarity. These similarity functions are integral to the optimization objective and play a key role in quantifying the relationships between nodes. All previously mentioned models (Ning et al. 2018; Song and Thiagarajan 2019; Ning et al. 2021b; Pio-Lopez et al. 2021; Zhang and Kou 2022; Luo et al. 2023) use the sigmoid as their similarity function $\varphi(v_i, v_j) = \sigma(\mathbf{c}_i^\top \mathbf{z}_j)$, where $\sigma(x) = 1/(1 + \exp(-x))$ and \mathbf{c}_i is the context vector

representation of v_i , and \mathbf{z}_j is the embedding of node v_j . [Huang et al. \(2021b\)](#) sort this similarity function into a class that they refer to as pointwise mutual information-based (PMI) functions. They examined the effect of using another type of similarity function called autocovariance ([Delvenne et al. 2013](#)), which they report outperformed PMI functions on link prediction tasks. Their analysis has never been extended to multiplex networks, and may be an interesting route for further research.

Embedding algorithm.

Finally, regarding the embedding algorithm, [Huang et al. \(2021b\)](#) distinguishes between matrix factorization and sampling techniques. We are only aware of negative sampling techniques being used on multiplex networks ([Zhang et al. 2018; Song and Thiagarajan 2019; Zhang and Kou 2022](#)). The idea behind negative sampling is to randomly select several elements outside the original dataset for each element within the dataset, aiming to improve the model's performance while maintaining computational efficiency. Most models work analogously to node2vec, and feed the node sequences to the Skip-Gram objective ([Mikolov et al. 2013a](#)) (see Equation (2)), which is then optimized using stochastic gradient descent ([Ning et al. 2018; Zhang et al. 2018; Chu et al. 2019; Song and Thiagarajan 2019; Wilson et al. 2021](#)). Since many of the real-world networks have a large number of nodes, it is intractable to optimize over all possible edges.

The Skip-gram algorithm with negative sampling ([Mikolov et al. 2013b](#)) achieves this by corrupting some of the existing edges and ensuring that these negative edges do not belong to the set of edges sampled during the random walk. This scheme is used to approximate the log of the conditional probability inside Equation (2), as computed by the Softmax, by:

$$\log p(v_{i+j}|v_i) = \log \sigma(\mathbf{c}_{i+j}^T \mathbf{z}_i) + b \cdot \mathbb{E}_{\mathbf{c} \sim p(\mathbf{c})} [\log \sigma(-\mathbf{c}^T \mathbf{z}_i)] ,$$

where the \mathbf{c} 's are context embeddings, $p(\mathbf{c})$ is the distribution from which the fake edges are sampled, and b is the number of negative samples. Another method to reduce the computational cost of the Softmax in the Skip-Gram is noise contrastive estimation (NCE) (Gutmann and Hyvärinen 2010), although it has not been used in multiplex network embedding. The NCE can be shown to approximately maximize the conditional log likelihood in the Skip-Gram objective, whereas the Skip-Gram with negative sampling is only a simplified version of NCE, based solely on heuristics (Mikolov et al. 2013b).

In models with layer-specific random walks, collaboration is achieved through the embedding algorithm. MNE (Zhang et al. 2018) facilitates this collaboration by replacing the enriched node embeddings with the sum of a shared representation across layers, combined with a transformation of the layer-specific embedding. The transformation function is learned during the optimization process. In OhmNet (Zitnik and Leskovec 2017), the layers are arranged hierarchically, reflecting the biological tissues considered. The algorithm is designed to convey hierarchical information as described by a tree, by ensuring that the node embeddings of replica nodes from parent and child networks are similar, as measured by the ℓ_2 -distance. Finally, in MVN2VEC-REG (Shi et al. 2018), layers are not hierarchically organized, but the representations specific to each layer are regularized by the average representation of replica nodes, thus, ensuring that the enriched embeddings are close to their mean value across replicas.

A very different approach is considered in MANE+ (Ata et al. 2021), where, in addition to the Skip-Gram objective for each layer, the model uses a Skip-Gram objective with interlayer connections. The goal is to capture what they refer to as first- and second-order collaboration in the multiplex network. These objective functions are summed to a final function.

The random walk approaches are popular for embedding learning on multiplex networks, which is reflected in their numerous publications. They are characteristically defined by their three-part structure, comprising a random process, a similarity function, and an embedding algorithm. This also separates them from the category of optimization methods, which is addressed below.

3.2.4 Optimization Methods

This section includes the remaining shallow methods that do not fit into the previous categories of matrix factorization and random walk-based approaches. The models in this section appear to share an underlying characteristic: each one is based on a direct pairwise comparison of node embeddings, aiming to preserve the similarities between the node pairs in the graph through some *first-order* or *second-order proximities*, as depicted in Figure 5. The k -order proximity refers to the k -step connection between nodes v_i and v_j , which can be measured by their transition probability $p^{(k)}(v_i, v_j) = [(\mathbf{D}^{-1}\mathbf{A})^k]_{ij}$ (Hou et al. 2020).

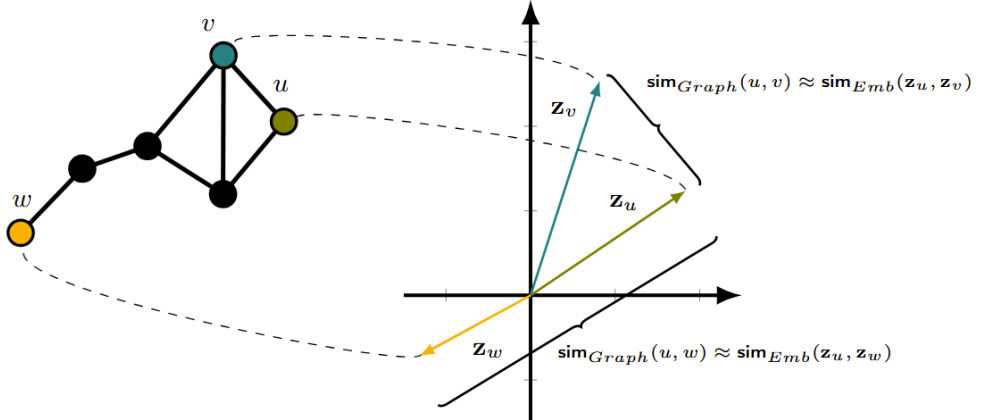


Figure 5: Optimization models mainly aim at preserving first-order and second-order proximity information, here on a monoplex network. This figure was inspired by Figure 2 in Baptista et al. (2023).

A prominent example on monoplex networks is LINE (Tang et al. 2015). This model focuses on preserving first-order and second-order proximities of a node by relying on prior-knowledge context embeddings $(\mathbf{c}_i)_{v_i \in V}$ and by maximizing over an objective function on the embedding matrix \mathbf{Z} for the proximity of order k on the monoplex network $\mathcal{G} = (V, E)$

$$\text{prox}^{(k)}(\mathbf{Z}; \mathcal{G}, (\mathbf{c}_i)_{v_i \in V}) = - \sum_{(v_i, v_j) \in E} p^{(k)}(v_i, v_j) \log p^{(k)}(v_i, v_j; \mathbf{Z}, (\mathbf{c}_i)_{v_i \in V}). \quad (5)$$

The predicted probability for the first-order proximity between nodes v_i and v_j with respective embeddings \mathbf{z}_i and \mathbf{z}_j is given by $p^{(1)}(v_i, v_j; \mathbf{Z}) = \sigma(\mathbf{z}_i^\top \mathbf{z}_j)$, where σ is the sigmoid function. On the other hand, the predicted probability of the second-order proximity uses the aforementioned context embedding \mathbf{c}_i for node v_i $p^{(2)}(v_i, v_j; \mathbf{Z}, (\mathbf{c}_i)_{v_i \in V}) = \sigma(\mathbf{c}_i^\top \mathbf{z}_j)$.

MTNE (Xu et al. 2018) extends the LINE model to multiplex networks by computing enriched embeddings. The authors facilitate collaboration between the layers through two distinct approaches. The first collaboration approach is by computing so-called common embeddings, which are representations shared across layers. These embeddings are obtained by maximizing over an objective function similar to Equation (5), where the first-order and second-order proximities are defined as

$$\begin{aligned} p^{(1)}(v_i^{[\alpha]}, v_j^{[\alpha]}; \mathbf{Z}) &= \sigma\left((\mathbf{z}_i^0 + \mathbf{z}_i^{[\alpha]})^\top (\mathbf{z}_j^0 + \mathbf{z}_j^{[\alpha]})\right) \\ p^{(2)}(v_i^{[\alpha]}, v_j^{[\alpha]}; \mathbf{Z}, (\mathbf{c}_i^\alpha)_{v_i \in V}) &= \sigma\left((\mathbf{c}_i^\alpha)^\top (\mathbf{z}_j^0 + \mathbf{z}_j^{[\alpha]})\right), \end{aligned}$$

where $\mathbf{Z}_0 = [\mathbf{z}_1^0, \dots, \mathbf{z}_N^0]^\top$ is the common embedding matrix, and \mathbf{c}_i^α is the context embedding associated with node v_i on layer α . Finally, the objective functions also include the Frobenius norms of each layer-specific concatenated embedding matrix

$((\mathbf{Z}_\alpha)_\alpha, (\mathbf{C}_\alpha)_\alpha)$ as regularization terms. The second collaboration approach taken in MTNE is to use the so-called consensus embeddings. The authors use the LINE algorithm on each layer, with an additional regularization term through a consensus matrix $\mathbf{K} \in \mathbb{R}^{N \times d}$ across layers such that the objective function includes $\sum_{\alpha \in Y} \|\mathbf{Z}_\alpha - \mathbf{K}\|_F^2 + \lambda \|\mathbf{K}\|_F^2$, where λ is a weighting parameter. This term forces the layer-specific embeddings to be more similar, thereby facilitating collaboration. On the task of link prediction, [Xu et al. \(2018\)](#) deduced from their experimental results that the common embedding approach mostly outperformed the consensus embedding one. They believed this was a result of the more explicit integration of layer-specific embeddings.

Another approach on multiplex networks, MELL ([Matsuno and Murata 2018](#)), also relies on a LINE-like strategy. However, contrary to MTNE, MELL uses separate head (source node) and tail (target node) embeddings, respectively denoted $(\mathbf{Z}_{\alpha,h})_\alpha, (\mathbf{Z}_{\alpha,t})_\alpha \subset \mathbb{R}^{N \times d}$. The purpose of this distinction was to better predict links in directed networks. Moreover, MELL also introduces layer embeddings $\mathbf{R} \in \mathbb{R}^{M \times d}$ to compute the first-order proximity: $p^{(1)}(v_i^{[\alpha]}, v_j^{[\alpha]}; \mathbf{Z}, \mathbf{R}) = \sigma((\mathbf{r}_\alpha + \mathbf{z}_{h,i}^{[\alpha]})^\top (\mathbf{z}_{t,j}^{[\alpha]}))$. Furthermore, [Matsuno and Murata \(2018\)](#) regularize the objective function to minimize the variances of the tail and head embedding matrices, to encourage embeddings from replica nodes to be more similar, akin to the consensus embeddings in MTNE. Then, the embeddings obtained with MELL belong to the class of numerous embeddings.

Another extension of LINE to multiplex networks is MVE ([Qu et al. 2017](#)), which assumes that $p^{(2)}(v_i^{[\alpha]}, v_j^{[\alpha]}; \mathbf{Z}, (\mathbf{c}_i)_{v_i \in V}) \propto \exp(\mathbf{c}_i^\top \mathbf{z}_j^{[\alpha]})$. Then the softmax value is heuristically approximated using the Skip-Gram with negative sampling objective ([Mikolov et al. 2013b](#)) in Equation (2). Finally, the objective function is regularized to force collaboration across the layers, with the term $\sum_{\alpha \in Y} \sum_{v_i \in V} \lambda_i^\alpha \|\mathbf{z}_i^{[\alpha]} - \mathbf{z}_i\|_2^2$, where λ_i^α are the weights indicating the influence of each node in each layer, and \mathbf{z}_i is the unique cross-layer embedding associated with node i , of the form $\mathbf{z}_i =$

$\sum_{\alpha \in Y} \lambda_i^\alpha \mathbf{z}_i^{[\alpha]}$. The $(\lambda_i^\alpha)_{v_i \in V, \alpha \in Y}$ are learned via an attention mechanism, using a version of the softmax function and optimized over the cosine similarities of the embedding vectors. [Qu et al. \(2017\)](#) found that their MVE model computes embeddings efficiently, performing comparably to LINE ([Tang et al. 2015](#)) and node2vec ([Grover and Leskovec 2016](#)).

Finally, another approach for multiplex networks which is distinct from LINE-like methods is MUNEM ([Hajiseyedjavadi et al. 2019](#)). At each epoch, [Hajiseyedjavadi et al. \(2019\)](#) sample triplets of nodes: an anchor node, a connected node, and an unconnected node, retrieved by corrupting the source node, and simultaneously optimize layer-specific and cross-layer objective functions over embeddings. The layer-specific objective function ensures that connected nodes are embedded closer to each other than unconnected nodes: $\mathcal{L}^{(\text{lay})}(\mathbf{Z}_\alpha) = \sum_{(v_a^{[\alpha]}, v_p^{[\alpha]}, v_n^{[\alpha]}) \in \mathcal{T}^\alpha} \max \left\{ 0, \|\mathbf{z}_a^{[\alpha]} - \mathbf{z}_p^{[\alpha]}\|_2^2 - \|\mathbf{z}_a^{[\alpha]} - \mathbf{z}_n^{[\alpha]}\|_2^2 + \delta_{in} \right\}$, where \mathcal{T}^α is the set of sampled triplets in layer α , and δ_{in} is a hyperparameter controlling the expected similarity between embeddings of connected versus unconnected nodes. The cross-layer objective function promotes collaboration among the different layers by sampling a triplet consisting of an anchor node, its replica node, and a unconnected node on the same layer: $\mathcal{L}^{(\text{cross})}(\mathbf{Z}_1, \dots, \mathbf{Z}_M) = \sum_{(v_a^{[\alpha]}, v_a^{[\beta]}, v_n^{[\beta]}) \in \mathcal{T}} \max \left\{ 0, \|\mathbf{z}_a^{[\alpha]} - \mathbf{z}_a^{[\beta]}\|_2^2 - \|\mathbf{z}_a^{[\alpha]} - \mathbf{z}_n^{[\beta]}\|_2^2 + \delta_{\text{bet}} \right\}$, where \mathcal{T} is the set of the aforementioned sampled triplets, and δ_{bet} is again a margin hyperparameter. Then, the final objective function in MUNEM is given by

$$\mathcal{L}(\mathbf{Z}_1, \dots, \mathbf{Z}_M) = \mathcal{L}^{(\text{cross})}(\mathbf{Z}_1, \dots, \mathbf{Z}_M) + \sum_{\alpha \in Y} \mathcal{L}^{(\text{lay})}(\mathbf{Z}_\alpha) .$$

Hajiseyedjavadi et al. (2019) acknowledge that sampling the entirety of possible connections is intractable, and suggest sampling only a portion of the links for computational efficacy, although they do not elaborate on the sampling scheme or the sampling size that should be used.

Most optimization methods generally operate on the definition of first-order and second-order proximities on the node pairwise comparison on embeddings. As illustrated in this section, this comparison typically resorts to the sigmoid function when using a probability-based approach, and a normed distance otherwise.

3.2.5 Neural Network-Based Methods

Artificial neural networks have become an exceptionally powerful and versatile framework for learning from data (Bishop and Bishop 2024). In particular, graph neural networks are neural networks applied to the graph domain (Zhou et al. 2020). Similarly to Han et al. (2021), we notice that some researchers attempt to extend single-layer neural network approaches to multiplex scenarios. Such approaches can be sorted into three categories (Ward et al. 2022): recurrent graph neural networks, graph convolution neural networks with spatial and spectral approaches, and graph autoencoders, including graph adversarial techniques.

Graph Convolution Neural Networks.

Graph convolutional neural networks (GCNs) resort to filtering around a neighborhood of nodes to compute node representations, in a manner similar to classical convolutional neural networks. At each iteration, the representation of a node is updated with the aggregation of the representations of neighboring (connected) nodes. Hence, graph neural networks inherit desirable properties from convolutional neural networks: locality, scalability, and interpretability (Ward et al. 2022). In Bielak and Kajdanowicz (2024), the corresponding aggregation step is called a GNN-level information fusion.

Unlike any of the other models presented in this paper, GNNs require an additional feature matrix $\mathbf{X} \in \mathbb{R}^{N \times F}$ for nodes. Then the triplet $\mathcal{M} = (Y, \mathcal{G}, \mathbf{X})$ defines an *attributed* multiplex network, such that a feature vector $\mathbf{x}_i \in \mathbb{R}^F$ is assigned to every node $v_i \in V$. The node feature matrix is typically used to initialize the recurrent computation of the embeddings, *i.e.*, the node feature vectors $\mathbf{x}_i \in \mathbb{R}^F$ are set as the initial embeddings $\mathbf{z}_i^{(0)} = \mathbf{x}_i$ and the resulting final embedding is typically set to the unique embedding of the node $\mathbf{z}_i = \mathbf{z}_i^{(L)}$, for a prespecified number of neural network layers $L \geq 0$. In what follows, we will distinguish between the multiplex network layer, which we will continue to denote by Greek letters, and neural network layers (NN-layer), which will be denoted by the index ℓ . Hence, the embedding of node v_i at NN-layer ℓ is given by $\mathbf{z}_i^{(\ell)}$. The formulation for the NN-layers is often written in terms of the embedding matrix, which is represented by $\mathbf{Z}^{(\ell)} = [\mathbf{z}_1^{(\ell)}, \dots, \mathbf{z}_N^{(\ell)}]^\top$ to simplify notation.

So far, all graph convolutional network (GCN)-based approaches for multiplex network embedding rely on two prominent monoplex models: GraphSAGE ([Hamilton et al. 2017](#)) and GAT ([Veličković et al. 2018a](#)).

GraphSAGE introduced a two-step process to compute the representation vectors for any node v_i at each NN-layer ℓ . First, a neighborhood embedding vector $\mathbf{z}_{\mathcal{N}(v_i)}^{(\ell)}$ is computed via an aggregation method applied to the neighborhood $\mathcal{N}(v_i)$ of node v_i . Then $\mathbf{z}_{\mathcal{N}(v_i)}^{(\ell)}$ and the embedding $\mathbf{z}_i^{(\ell-1)}$ of node v_i at NN-layer $\ell - 1$ are jointly transformed, and run through a nonlinear activation function. Formally, for a node v_i at NN-layer ℓ , the steps are given by

$$\begin{aligned} (1) \quad & \mathbf{z}_{\mathcal{N}(v_i)}^{(\ell)} = \text{Agg}_\ell \left(\{\mathbf{z}_j^{(\ell-1)}; v_j \in \mathcal{N}(v_i)\} \right) \\ (2) \quad & \mathbf{z}_i^{(\ell)} = \text{act}_\ell \left(\mathbf{W}_\ell \cdot \text{concat} \left(\mathbf{z}_i^{(\ell-1)}, \mathbf{z}_{\mathcal{N}(v_i)}^{(\ell)} \right) \right), \end{aligned}$$

where Agg_ℓ is the differentiable aggregation method for NN-layer ℓ , act_ℓ is the activation function at NN-layer ℓ , concat is the operator for concatenation, and finally, $\mathbf{W}_\ell \in \mathbb{R}^{d_\ell \times 2d_{\ell-1}}$ is the weight matrix for NN-layer ℓ with d_ℓ the dimension of the ℓ^{th} NN-layer. Then, [Hamilton et al. \(2017\)](#) give three examples of aggregation functions: the mean aggregator, the LSTM aggregator, and the pooling aggregator.

[Veličković et al. \(2018a\)](#) take a different approach, they design a graph attention mechanism that learns the importance of each node within its corresponding neighborhood. Their method GAT achieves this by first running a self-attention NN-layer on each node embedding, and then, for each edge (v_i, v_j) , taking the softmax of the attention coefficients over all edges involving v_i .

$$\lambda_{i,j} = \text{Softmax}(\text{att}(\mathbf{W}\mathbf{z}_i, \mathbf{W}\mathbf{z}_j)) = \frac{\exp(\text{att}(\mathbf{W}\mathbf{z}_i, \mathbf{W}\mathbf{z}_j))}{\sum_{v_k \in \mathcal{N}(v_i)} \exp(\text{att}(\mathbf{W}\mathbf{z}_i, \mathbf{W}\mathbf{z}_k))},$$

where $\mathbf{W} \in \mathbb{R}^{d \times F}$ is the weight matrix of the attention mechanism, and att is the attention function. Then, the resulting embedding for node v_i is given by $\mathbf{z}_i^{(1)} = \text{act}\left(\sum_{v_j \in \mathcal{N}(v_i)} \lambda_{ij} \mathbf{W}\mathbf{z}_j\right)$. To stabilize training, the authors suggest computing the self-attention layer multiple times independently to average the attention. They refer to this procedure as multi-head self-attention.

GraphSage and GAT have been extended to multiplex networks through MultiplexSAGE ([Gallo et al. 2024](#)) and MGAT ([Xie et al. 2020](#)), respectively.

In MultiplexSAGE, [Gallo et al. \(2024\)](#) implement collaboration by using an aggregation function to fuse intra- and interlayer neighborhood information into the node representation at NN-layer ℓ . That is

$$\mathbf{z}_i^\ell = \text{Agg}_\ell \left(\left\{ \mathbf{z}_j^{(\ell-1)} \mid \forall v_j \in \mathcal{N}_H(v_i) \right\} \cup \left\{ \mathbf{z}_j^{(\ell-1)} \mid \forall v_j \in \mathcal{N}_V(v_i) \right\} \cup \{ \mathbf{z}_i^{(\ell-1)} \} \right), \quad (6)$$

where $\mathcal{N}_H(v_i)$ and $\mathcal{N}_V(v_i)$ are the intra- and interlayer neighborhoods of v_i . Finally, the embedding of node v_i at NN-layer ℓ in MultiplexSAGE is given by

$$\mathbf{z}_i^{(\ell)} = \text{act} \left(\mathbf{W}_H^\ell \cdot \sum_{v_j \in \mathcal{N}_H(v_i)} \frac{\mathbf{z}_j^{(\ell-1)}}{|\mathcal{N}_H(v_i)|} + \mathbf{W}_V^\ell \cdot \sum_{v_j \in \mathcal{N}_V(v_i)} \frac{\mathbf{z}_j^{(\ell-1)}}{|\mathcal{N}_V(v_i)|} + \mathbf{S}^\ell \mathbf{z}_i^{(\ell-1)} \right), \quad (7)$$

where \mathbf{W}_H^ℓ , \mathbf{W}_V^ℓ , and \mathbf{S}^ℓ are the respective weight matrices for the NN-layer ℓ . However, MultiplexSAGE is more appropriate for multilayer networks than for multiplex networks, since the last two terms in the sum of Equation (7) boil down to $(\mathbf{W}_V^\ell + \mathbf{S}^\ell) \mathbf{z}_i^{(\ell-1)}$ for multiplex networks (Kivelä et al. 2014). Moreover, Equation (6) can also be simplified to $\mathbf{z}_i^{(\ell)} = \text{Agg} \left(\left\{ \mathbf{z}_j^{(\ell-1)} \mid \forall v_j \in \mathcal{N}_H(v_i) \right\} \cup \{ \mathbf{z}_i^{(\ell-1)} \} \right)$ in multiplex networks. This considerably differs from GraphSAGE, because the embedding from the previous NN-layer is also included in the aggregation step in MultiplexSAGE. The experiments in Gallo et al. (2024) show that GraphSAGE generally outperformed its multiplex counterpart for intralayer link prediction, emphasizing the importance of good integration of the inter- and intralayer information. More refined extensions of GraphSAGE to multiplex networks have been developed to overcome this issue. For instance, CGNN (Ren et al. 2024) uses a very similar approach to MultiplexSAGE but is restricted to two-layered multiplex networks. In matrix form, their aggregation step is written as

$$\mathbf{Z}_\alpha^\ell = \text{act} \left(\mathbf{Z}_\alpha^{(\ell-1)} \mathbf{W}_1^\ell + \mathbf{D}_\alpha^{-1/2} \mathbf{A}_\alpha \mathbf{D}_\alpha^{-1/2} \mathbf{Z}_\alpha^{(\ell-1)} \mathbf{W}_2^\ell + \mathbf{B}^\ell \mathbf{Z}_\beta^{(\ell-1)} \mathbf{W}_3^\ell \right),$$

where the elements of the matrix \mathbf{B}^ℓ are given by $[\mathbf{B}^\ell]_{ij} = \sigma(\mathbf{z}_i^{(\ell-1)\top} \mathbf{z}_j^{(\ell-1)})$, with \mathbf{B}^0 being the null matrix. Then, the parameters in CGNN are optimized over an intralayer information-related objective function, given by the sum of the layer Skip-Gram objective (Equation (2)) and an interlayer objective function. This objective

function pushes embeddings of replica nodes closer together while pulling embeddings of non-replica nodes apart using the cosine similarity.

On the other hand, MGAT (Xie et al. 2020) extends GAT (Veličković et al. 2018a) to a multiplex context. MGAT computes a layer-specific multihead self-attention mechanism, which forces the weight matrices $(\mathbf{W}_\ell)_\ell$ to be similar across NN-layers k, ℓ by including the sum over all possible weight differences $\|\mathbf{W}_k - \mathbf{W}_\ell\|_2^2$ in the objective function. To construct a unique node embedding from these layer-specific representations, they again use an attention mechanism, where a coefficient $\eta_{\alpha,i}$ associated with layer α and node v_i is computed as $\eta_{\alpha,i} = \text{Softmax}(\mathbf{t}_\alpha^\top (\text{concat}_{\alpha \in Y} \mathbf{z}_i^{[\alpha]}))$ over the set of replica nodes of v_i in the multiplex graph. In this equation, $\text{concat}_{\alpha \in Y} \mathbf{z}_i^{[\alpha]} \in \mathbb{R}^{Md}$ is the concatenation of the layer-specific embeddings, and $\mathbf{t}_\alpha \in \mathbb{R}^{Md}$ is a trainable parameter for layer α . Then, unique node embeddings are retrieved by taking the linear combination of the node v_i 's representations across layers by $(\eta_{\alpha,i})_\alpha$'s. Figure 6 displays the architecture of MGAT.

In a related work, named LIAMNE (Chen et al. 2024), the layer attention coefficient is computed as $a_i = \mathbf{w}_1^\top \tanh(\mathbf{W}_2 \cdot \text{concat}_{\alpha \in Y} \mathbf{z}_i^{[\alpha]})$, where $\mathbf{w}_1 \in \mathbb{R}^{Md}$ and $\mathbf{W}_2 \in \mathbb{R}^{N \times Md}$ are trainable parameter vectors and matrices, respectively. The $\mathbf{z}_i^{[\alpha]}$ in the equation are computed using the GraphSAGE mean aggregator method to node v_i in layer α . The final enriched embeddings are retrieved by a learnable affine combination of the final layer-specific embedding $\mathbf{z}_i^{[\alpha],(L)}$ and the $\text{concat}_{\alpha \in Y} \mathbf{z}_i^{[\alpha]}$. Moreover, Chen et al. (2024) also discuss the problem of handling *layer imbalance* on multiplex networks, that is, the discrepancy in the number of edges across layers. This discrepancy may lead to learning bias and performance degradation on the most sparse layers. Chen et al. (2024) addresses this issue by first constructing a new multiplex network through a sampling scheme that retains the full target layer but undersamples auxiliary layers, on which LIAMNE is applied.

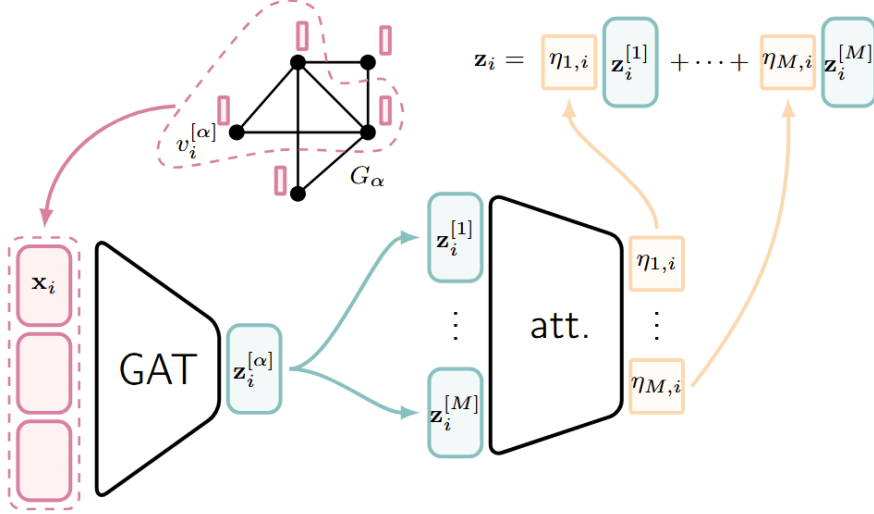


Figure 6: The MGAT algorithm (Xie et al. 2020). First, the 1-step neighbors to node v_i are retrieved. Then, the attribute vectors from all neighbors are merged into a layer-specific representation $h_i^{[\alpha]}$. Using an attention mechanism, the relevance of each layer-specific representation is concentrated in the $\eta_{\alpha,i}$ coefficients, which are the coefficients of the linear combination of neighbor embeddings yielding the final node embedding.

mGCN (Ma et al. 2019) takes a different approach to implementing the layer attention mechanism than MGAT and LIAMNE. For each node, mGCN maintains at the same time a layer-specific embedding matrix $\mathbf{Z}_\alpha^{(\ell)}$ for each layer α and a common embedding matrix $\mathbf{Z}^{(\ell-1)}$ across layers, and then alternately updates them. The layer-specific embedding matrix is obtained from the common embedding matrix with the operation $\mathbf{Z}_\alpha^{(\ell)} = \text{act}(\mathbf{W}_\alpha \mathbf{Z}^{(\ell-1)})$; the common embedding matrix is conversely updated with $\mathbf{Z}^{(\ell)} = \text{act}(\mathbf{W} \text{concat}_{\alpha \in Y} \mathbf{Z}_\alpha^{(\ell-1)})$. Moreover, $\mathbf{Z}_\alpha^{(\ell)}$ is updated for each layer α by the convex combination of $\mathbf{Z}_\alpha^{(\ell)}$ multiplied by the row-normalized adjacency matrix with self-loops $\hat{\mathbf{A}}_\alpha = \mathbf{D}_\alpha^{-1}(\mathbf{A}_\alpha + \mathbf{I})$, and the result of the attention mechanism with the attention function $\text{tr}(\mathbf{W}_\alpha^\top \mathbf{M} \mathbf{W}_\beta)$. Note that the attention mechanism is applied to the weight matrices $\mathbf{W}_\alpha, \mathbf{W}_\beta$ instead of the intermediate embeddings \mathbf{z}_α^ℓ , as in previous models.

Among the methods described in this section, we could have made a distinction between spatial and spectral methods. However, we believe our presentation enables us to better capture the similarities among the different models. Note that models using the structure $\mathbf{Z}^{(\ell)} = \text{act}(\hat{\mathbf{A}}\mathbf{Z}^{(\ell-1)}\mathbf{W})$ are all linear approximations of Chebyshev polynomial filters in the spectral domain, with a constrained number of free parameters (Kipf and Welling 2017). As such, they demonstrate an equivalence with the spatial approach described, for instance, in Ward et al. (2022). The renormalization $\hat{\mathbf{A}}$ of the adjacency matrix with self-loops is a simplification of the technically correct result $\mathbf{I} + \mathbf{D}^{-1/2}\mathbf{A}\mathbf{D}^{-1/2}$. This simplification avoids numerical instabilities as a result of exploding or vanishing gradients during the optimization process (Defferrard et al. 2016).

Adversarial Networks

Generative adversarial networks (GANs) implement a *minimax* game in which a generator, typically referred to with the letter \mathbb{G} , generates data to trick a discriminator, referred to with the letter \mathbb{D} , which determines whether the data is true or not.

The application of adversarial networks to representation learning on monoplex networks was initiated by GraphGAN (Wang et al. 2017). GraphGAN implements a generator that produces node embeddings, and a discriminator for inferring whether an edge is present in the network using the generated embeddings. The probability of an edge (v_i, v_j) is the product of the sigmoid function applied on the dot product of the corresponding embeddings \mathbf{z}_i and \mathbf{z}_j : $\mathbb{D}(v_i, v_j) = \sigma(\mathbf{z}_i^\top \mathbf{z}_j)$. However, the definition of the generator is more sophisticated. Wang et al. (2017) construct a more computationally efficient graph-specific approximation of the softmax operator, which they refer to as Graph-Softmax. Finally, the goal is to find the respective parameters $\theta_{\mathbb{G}}$ and $\theta_{\mathbb{D}}$ of the generator and the discriminator that are solution to the following

optimization problem

$$\min_{\theta_G} \max_{\theta_D} \mathcal{V}(G, D) := \sum_{i=1}^N \mathbb{E}_{v \sim p_*(v_i)} [\log D(v, v_i; \theta_D)] + \mathbb{E}_{v \sim p_G(v_i; \theta_G)} [\log(1 - D(v, v_i; \theta_D))], \quad (8)$$

where $p_*(v)$ and $p_G(v; \theta_G)$ are, respectively, the true and the generated connectivity distribution on edges involving node v . The solutions to the two-player minimax game are iteratively updated until they converge to a stable solution. However, this convergence is not guaranteed, even if regularization might help (Mescheder et al. 2018).

Now, we consider extensions of GraphGAN to multiplex networks.

Since the Graph-Softmax cannot easily be generalized to multiplex networks, the authors of MEGAN (Sun et al. 2019) resorted to another architecture for the generator G . First, a generator fuses the representations of two nodes together, and computes from that representation the layer-specific probability that the corresponding nodes are connected. The product of these probabilities across the multiplex layers is evaluated to obtain a final probability value indicating whether the two nodes are connected. Then, similarly to the Graph-Softmax approach in GraphGAN, MEGAN reduces the computational complexity by restricting negative samples to a neighborhood of the source node. The neighborhood of a node v_i is defined as the set of replica nodes that are connected to v_i : $\mathcal{N}(v_i) = \{v_i \in V \mid \exists \alpha \in Y : (v_i^{[\alpha]}, v_j^{[\alpha]}) \in E_\alpha\}$. The resulting objective function for MEGAN is similar to Equation (8) in GraphGAN.

Another extension, VANE (Fu et al. 2020), solves a different adversarial game. VANE applies two simultaneous games, each with three players. The first game includes the players (1) F_N , which is a fully connected layer for one-hot encoded vectors; (2) a long-short-term memory model (LSTM) (Hochreiter and Schmidhuber 1997) F_S , which takes in the node embeddings of a sequence of nodes S sampled through a multiplex layer-specific random walk, and returns a subgraph representation \mathbf{z}_S ; (3) the discriminator D_S takes in the subgraph embedding and predicts

the layer the subgraph lies in. Together, F_N and F_S extract multiplex unique node embedding representations. The game is characterized by the optimization problem $\min_F \max_{\mathbb{D}_S} \mathbb{E}_{\mathbf{z}_S \sim p_\alpha(\mathbf{z}_S)} [\log \mathbb{D}_S(\mathbf{z}_S)] + \mathbb{E}_{\mathbf{z}_S \sim \bar{p}_\alpha(\mathbf{z}_S)} [\log(1 - \mathbb{D}_S(\mathbf{z}_S))]$, where $p_\alpha(\mathbf{z}_S)$ is the distribution of the subgraph representation for layer α and $\bar{p}_\alpha(\mathbf{z}_S)$ is the distribution for the layers other than α . The second game includes the players \mathbb{G} , a generator that constructs fake node representations. F_N , the same player as in the first game, is an embedder that helps the discriminator \mathbb{D}_N to distinguish between valid and generated embeddings. The second game is determined by

$$\min_G \max_{F_N} \max_{\mathbb{D}_N} \mathbb{E}_{F_N(V) \sim p(F_N(v))} [\log \mathbb{D}_N(F_N(v))] + \mathbb{E}_{\mathbf{z} \sim p_\mathbf{z}(\mathbf{z})} [\log(1 - \mathbb{D}_N(\mathbb{G}(\mathbf{z})))],$$

where $p_\mathbf{z}(\mathbf{z})$ is a noise distribution and p is the generated distribution. Contrary to MEGAN, which iterates the game until convergence, VANE iterates the game for a predetermined number of sampled node sequences.

A somewhat different approach to classical adversarial games on monoplex networks like GraphGAN is taken in DGI ([Veličković et al. 2018b](#)). First, node embeddings $(\mathbf{z}_i)_{v_i \in V}$ are generated using a GCN. Second, representations $(\tilde{\mathbf{z}}_i)_{v_i \in V}$ on a corrupted version of the network and node attributes are obtained through the same GCN. Third, a graph representation s is computed by taking the sigmoid of the average of all true node representations, $\mathbf{s} = \sigma(\frac{1}{N} \sum_{v_i \in V} \mathbf{z}_i)$. Finally, the discriminator $\mathbb{D}(\mathbf{z}; \mathbf{s}) = \sigma(\mathbf{z}^\top \mathbf{W} \mathbf{s})$ takes in a node embedding \mathbf{z} and outputs the probability of the embedding being valid. The objective function is the cross-entropy loss between predictions made on the true node representation \mathbf{z}_i and the corrupted one $\tilde{\mathbf{z}}_i$ for each node $v_i \in V$.

A variant of DGI (called MNI-DGI) for multiplex networks is introduced in [Wang et al. \(2023\)](#), which applies DGI layer-wise and defines an objective function called Infomax, that maximizes mutual information to achieve collaboration between the

layers. Note that this model does not fall into the category of aggregation methods, because the Infomax approach is not applied retrospectively. Another extension of DGI to multiplex networks is DMGI (Park et al. 2020). DMGI applies the DGI model separately to each layer of the multiplex and fosters interlayer collaboration through two techniques. First, DMGI defines a single discriminator common to all layers, and second, the authors introduce a consensus matrix-type technique, similar to that introduced in Section 3.2.4 for the MTNE model (Xu et al. 2018). The loss function (to minimize) is defined as

$$\mathcal{L}(\mathbf{K}, \mathbf{Z}_1, \dots, \mathbf{Z}_M, \tilde{\mathbf{Z}}_1, \dots, \tilde{\mathbf{Z}}_M) = \left[\mathbf{K} - \frac{1}{M} \sum_{\alpha \in Y} \mathbf{Z}_\alpha \right]^2 - \left[\mathbf{K} - \frac{1}{M} \sum_{\alpha \in Y} \tilde{\mathbf{Z}}_\alpha \right]^2,$$

where $\mathbf{K} \in \mathbb{R}^{N \times d}$ is the consensus matrix across layers, $(\mathbf{Z}_\alpha)_{\alpha \in Y}$ are the true and $(\tilde{\mathbf{Z}}_\alpha)_{\alpha \in Y}$ are the corrupted layer-specific embedding matrices. As a result, the objective function minimizes the disagreement between the consensus matrix and the true embedding matrices, while maximizing the difference with the corrupted node embeddings. Park et al. (2020) also present a version of the DMGI model that utilizes an attention mechanism, as opposed to the consensus approach, where the attention mechanism for node v_i is defined by the softmax function $a_i = \text{softmax}(\mathbf{t}_\alpha^\top \mathbf{z}_i^{[\alpha]})$. Again, \mathbf{t}_α is a trainable parameter for layer α . Park et al. (2020) deduce from their experiments that the attention mechanism generally outperforms the consensus approach. Another work building upon DGI, HMNE (Ning et al. 2021a) exists but is out of scope for our review, as it was never applied to a link prediction task.

As a conclusion, first, most of the models in this section merely extend approaches on monoplex networks to multiplex networks. Second, most of those models use unique embeddings. The only exceptions to this rule are LIAMNE (Chen et al. 2024), CGNN (Ren et al. 2024) and MNI-DGI (Wang et al. 2023), which generate enriched embeddings. Third, several graph convolutional neural networks have

been proposed for clustering and classification tasks, including MAGCN (Yao et al. 2022), MGCN (Ghorbani et al. 2018), Multi-GCN (Khan and Blumenstock 2019), and MR-GCN (Huang et al. 2021a). We claim that, with only minor adjustments, these networks could also be used for link prediction. Fourth, we were unable to find autoencoder models specifically designed for multiplex or attributed multiplex networks, which paves the way for novel interesting research. Finally, many neural network models are not designed for *weighted* multiplex networks, and therefore, their performance in these scenarios cannot be assessed.

4 Link Prediction Evaluation

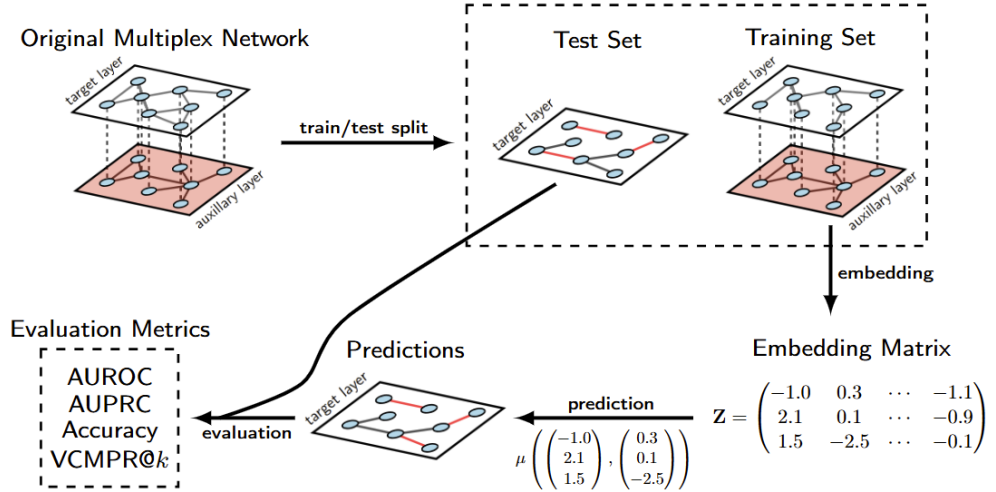


Figure 7: This figure visualizes the evaluation procedure for layer-specific testing procedures. The grey lines in the target layer represent true edges (resp. predicted true edges), whereas the red lines represent the false edges (resp. predicted false edges). The predictor μ takes in two vector representations, i.e. columns from the embedding matrix \mathbf{Z} .

As previously mentioned, link prediction aims to infer edges or estimate their weights in a (multiplex) network. Various factors can influence the performance of link prediction models, and many of these are designed for specific use cases. Consequently,

a wide range of evaluation methods has emerged, one of which is visualized in Figure 7, making it challenging to compare results across different studies. In this section, we will outline the possible choices for embedding dimensions, prediction methods, evaluation metrics, and testing procedures. We leave out a discussion on the datasets, as the review by [Han et al. \(2021\)](#) on embedding models for clustering on multiplex networks already describes the most prominent choices for multiplex networks.

4.1 Embedding Dimension

Multiplex networks may exhibit various sizes, ranging from 29 nodes and three layers, as in the Vickers dataset ([Vickers and Chan 1981](#)), to over 400,000 nodes and two layers, as in the Twitter dataset ([Domenico et al. 2013](#)). Criterion **(iv)** from Section 3.1 requires an efficient embedding model to map the nodes into a low-dimensional latent space, where the dimension d should be chosen to be much smaller than the number of nodes N . Typically, the dimension d of the embedding space is set prior to training. Most publications set d to 64 or 128 for large networks ([Zitnik and Leskovec 2017](#); [Sun et al. 2019](#); [Ning et al. 2020](#); [Pio-Lopez et al. 2021](#); [Du et al. 2022](#); [Wang et al. 2023](#); [Chen et al. 2024](#)). Some of the authors argue that fixing the dimension beforehand allows for a better comparison across models ([Matsuno and Murata 2018](#); [Ma et al. 2019](#); [Ata et al. 2021](#)). In contrast, [Gu et al. \(2021\)](#) mention that the embedding dimension is sometimes also learnt as a hyperparameter for single-layer network approaches.

However, the choice of d does not seem to be the driving factor for the quality of the latent vector representation, as long as it is large enough. Some authors tested the performance of their model for various sizes, and found no significant improvements beyond $d = 16$ or $d = 40$ ([Wilson et al. 2021](#); [Wang et al. 2023](#)). In monoplex networks, [Gu et al. \(2021\)](#) shows that node2vec ([Grover and Leskovec 2016](#)) and LINE ([Tang et al. 2015](#)) achieve little to no improvement with dimensions greater than $d = 10$ or $d = 45$. Interestingly, [Ning et al. \(2021b\)](#) empirically tested their models

FFME and MHME over a range of different embedding dimensions, and observed a significant increase in performance up to $d = 100$, although the performance improvement was lesser past $d = 50$. The performance of LIAMNE (Chen et al. 2024) even dropped past $d = 64$.

As a result, some care should be taken when choosing the embedding dimension. Gu et al. (2021) suggest a principled approach to determine the best embedding size for link prediction in monoplex networks. The lack of theoretical underpinning shows that more research is needed on that front. Moreover, it is unknown how well this approach translates to multiplex networks.

4.2 Prediction Method

After the embedding learning phase, d -dimensional node embeddings can be fed to a classifier or a regression tool to make predictions about missing edges in the network. Two approaches are mainly used for predicting intralayer edges: either similarity-based or machine learning-based methods. Similarity-based approaches return a scalar value for each pair of nodes based on their embeddings, whereas machine learning-based methods jointly transform the node embeddings corresponding to the edge, and feed the resulting edge embedding to a downstream ML model. The expression of the two main prediction methods is provided in Table 2. In either case, the perspective on whether the embeddings represent points or vectors in space is of fundamental importance. Every vector in a Euclidean space is characterized by two points therein; as such, each point can be considered as a vector through the origin. However, one might wonder whether the angle, the specific location in space, or a mixture of these is most relevant for inferring edges.

Among similarity-based approaches, the most common one is the cosine similarity (Zhang et al. 2018; Hajiseyedjavadi et al. 2019; Fu et al. 2020; Xie et al. 2020; Wang et al. 2023). Cosine similarity takes the embeddings of two nodes, and computes

Method	Formula
Cosine Similarity Hadamard Product + Classifier/Regressor	$\cos(v_i, v_j) = \mathbf{z}_i^\top \mathbf{z}_j / (\ \mathbf{z}_i\ \ \mathbf{z}_j\)$ $\mathbf{z}_i \odot \mathbf{z}_j = ([\mathbf{z}_i]_1 \cdot [\mathbf{z}_j]_1, \dots, [\mathbf{z}_i]_N \cdot [\mathbf{z}_j]_N)^\top$

Table 2: Main prediction methods for edge presence and edge weight inference in multiplex networks.

the cosine value of the angle between them. Therefore, it falls under the methods that neglect the magnitudes of these vectors. The cosine similarity has values in $[-1, 1]$, where a value of 1 (resp., -1) is achieved for collinear vectors of the same (resp., opposite) direction. Hence, a computed value closer to 1 infers an edge between the nodes. While the cosine similarity is the most popular approach for link prediction in monoplex and multiplex networks, there are growing concerns about its effectiveness due to omitting the information related to the magnitudes (Zhou et al. 2022; Steck et al. 2024; You 2025). Because of this, the similarities calculated by cosine similarity might be meaningless (Steck et al. 2024).

Machine learning-based edge prediction methods appear less popular, as they are less frequently cited in papers. Nevertheless, some authors use a logistic regression or a random forest classifier on a transformation of the pair of embeddings to predict corresponding edges (Ma et al. 2019; Zhang and Kou 2022; Ren et al. 2024). Furthermore, these models usually take the Hadamard product of the two nodes as their input, as first introduced in Grover and Leskovec (2016), that is, the element-wise multiplication of the two node embeddings associated with the evaluated edge. How the machine learning prediction methods compare to the more popular cosine similarity remains to be assessed.

Lastly, for the sake of comparability between models, we suggest that the approach should be chosen to work on all types of networks, be it (un)directed and (un)weighted, for the sake of having a reliable predictor on all types of layers.

4.3 Evaluation Metrics

Metric	Formula
Precision	$TP / (TP + FP)$
Accuracy	$(TP + TN) / (TP + TN + FP + FN)$
F1-Score	$(2 \cdot TP) / (2 \cdot TP + FP + FN)$
VCMPR@k	$t_{v_i}(k) / \min\{\deg(v_i), k\}$
NRMSE	$\sqrt{\frac{1}{ D } \sum_{y \in D} \hat{y} - y ^2 / \max \hat{y} - y }$

Table 3: Metrics for evaluating performance in link prediction. TP: number of true positive edges. FP: number of false positive edges. TN: number of true negative edges. FN: number of false negative edges.

The most commonly used metrics for link prediction on multiplex networks are the area under the receiver-operator curve (AUROC) (Qu et al. 2017; Matsuno and Murata 2018; Ning et al. 2018; Xu et al. 2018; Ma et al. 2019; Fu et al. 2020; Xie et al. 2020; Wang et al. 2023; Chen et al. 2024), the area under the precision-recall curve (AUPRC) (Shi et al. 2018; Wang et al. 2023), the average precision (Sun et al. 2019), the accuracy (Liu et al. 2017), and the F1 (Liu et al. 2017) scores. The definition of some metrics is recalled in Table 3. Note that all these metrics are classical performance measures for binary classification problems (Rainio et al. 2024).

In representation learning in monoplex networks, some researchers have started to question those metrics, and whether they reflect the performance of models in sparse networks. Lichtenwalter and Chawla (2012) and Menand and Seshadri (2024) argue that the class imbalance—that is, the discrepancy in numbers—between present and absent edges in sparse networks yields a bias in the evaluation using the classical binary classifier metrics. Lichtenwalter and Chawla (2012) also discuss the difficulty of accurately evaluating directed networks. These concerns also apply to multiplex networks. (Menand and Seshadri 2024) concluded that the prediction performance

should be evaluated at a vertex level. Both [Lichtnwalter and Chawla \(2012\)](#); [Menand and Seshadhri \(2024\)](#) have received little attention so far, yet they emphasize an important issue in the field.

Finally, link prediction on weighted networks has been utterly overlooked to date. A simple approach would use the ℓ_2 -norm, and perform evaluation with the Root Mean Squared Error (RMSE), in an analogy to classical regression problems.

4.4 Testing Procedure

Finally, the last crucial step to evaluate an embedding learning model is to construct a testing pipeline. An important part of the evaluation procedure is to construct appropriate training and testing sets from multiplex networks. We can generally distinguish between *general* ([Matsuno and Murata 2018](#); [Ning et al. 2018](#)) and *layer-specific* ([Hajiseyedjavadi et al. 2019](#); [Ma et al. 2019](#); [Xie et al. 2020](#); [Wang et al. 2023](#)) procedures.

In general procedures, the multiplex network is assumed to be the ground truth. Then, a set of false edges is generated via a random sampling scheme ([Matsuno and Murata 2018](#); [Ning et al. 2018](#)). In the sampling scheme, false edges e' are sampled uniformly from the set of non-existing edges, *i.e.*, $e' \sim \mathcal{U}(\bigcup_{\alpha \in Y} (V_\alpha \times V_\alpha) \setminus (L_\alpha \cup E_\alpha))$, where $\mathcal{U}(\cdot)$ represents the uniform distribution and $L_\alpha = \{(v_i^{[\alpha]}, v_i^{[\alpha]}) \mid i = 1, \dots, N\}$ the set of self-loops. Then, the set of all true and false intralayer edges of the network is divided into training, validation, and testing sets. A reduced multiplex network is constructed from the training set of true edges, which is subsequently used to train the embedding learning model. The latent vector pairs for the respective true and false edges of the test set are used to evaluate the prediction method. There are a few adaptations to this procedure. [Fu et al. \(2020\)](#) go a step further, and split the data on edges that exist across all layers and replica nodes. In contrast, [Ma et al. \(2019\)](#)

adapt the general approach by removing edges between node pairs from the training set at every layer.

Contrary to the general approach, the layer-specific procedure splits the multiplex network into a *target layer*, whose edges are split into training, validation, and test sets, and *complementary layers* (also known as *auxiliary layers* (Chen et al. 2024)), which remain unchanged. The complementary layers are used to provide additional information that enhances predictions on the target layer. The false edge sampling scheme for the training and testing sets follows the same procedure as above, although it is limited to the target layer, as depicted in Figure 7. This procedure offers a significant benefit over the previous one by iteratively choosing each layer in a multiplex network as the target layer, thereby measuring layer-dependent performance.

Those same procedures have been used to evaluate models on directed networks (Matsuno and Murata 2018; Xie et al. 2020). However, we would like to point out that the likelihood of sampling every edge's reciprocal is small, as most real-world networks exhibit sparsity (Boccaletti et al. 2014; Kivelä et al. 2014; Bianconi 2018). We can formally show this by assuming $E \subset V \times V \setminus L$ with $E \neq \emptyset$ and $\#E \ll \#[(V \times V) \setminus L] = \#V \cdot (\#V - 1)$, where L is the set of self-loops. Then we define the set of negative reciprocal edges $E_r := \{(v_i, v_j) \in V \times V \setminus L \mid (v_i, v_j) \notin E \text{ and } (v_j, v_i) \in E\}$, for which we clearly have the property $\#E_r \leq \#E$ and $\#L = \#V$. The probability of sampling a reciprocal false edge is now bounded by the probability of sampling a true edge, which is much smaller than sampling from the remaining false edges. In mathematical terms, for an edge $e \in V \times V \setminus L$

$$\mathbb{P}(e \in E_r) = \frac{\#E_r}{\#V \cdot (\#V - 1)} < \frac{\#(E_r \cup E)}{\#V \cdot (\#V - 1)} \ll 1 - \frac{\#(E_r \cup E)}{\#V \cdot (\#V - 1)} = \mathbb{P}(e \notin E_r \cup E).$$

Since edges in $[(V \times V) \setminus L] \setminus (E \cup E_r)$ have a weight equal to zero in both directions, these edges behave essentially as undirected edges. This effect may artificially inflate

the model’s performance during evaluation on directed networks when using symmetric predictions.

Therefore, we suggest instead another two-part testing procedure for directed multiplex networks. In the first test, the false edges are simply the non-existing reciprocal edges. This testing scheme may allow us to determine whether a model can accurately predict the directionality of those edges. The second test samples false edges uniformly from the set $[(V \times V) \setminus L] \setminus (E_r \cup E)$. This scheme may indicate whether using numerous embeddings performs worse than enriched embeddings when the directionality of these false edges is irrelevant.

5 Conclusion

Embedding methods map nodes to low-dimensional Euclidean spaces to perform downstream tasks such as link prediction. In this paper, we focused on the specific challenges linked to multiplex networks, and extended a model taxonomy for monoplex networks. Then, we leveraged this taxonomy to classify and compare embedding learning models from the literature. We found that many of the models are actually extensions of methods applied to monoplex networks, with additional constraints to achieve collaboration across layers. Furthermore, we introduced a new taxonomy specific to multiplex embedding: the representation taxonomy. This taxonomy enables a more structured comparison of the models. Beyond the taxonomies, we provide an overview of the current approaches to evaluating multiplex network embedding models. Finally, we proposed a new testing procedure for directed multiplex networks, to counteract the shortcomings of the currently used testing schemes.

The field of embedding learning on multiplex networks is still relatively new and remains an actively studied area. Therefore, many avenues of research remain unexplored, some of which we highlighted in our review, making it a promising field of research with clear real-life applications.

Declarations

Conflict of Interest: The authors have no relevant financial or non-financial interests to disclose.

Funding: No funding was received to assist with the preparation of this manuscript.

Author Contributions Statement: O.T. has designed the review and wrote the manuscript's text, tables and figures. O.W. has given substantial proof-reading to the manuscript. C.R. has supervised the review and co-wrote the text. All authors reviewed the manuscript.

References

Achour O, Romdhane LB (2025) A theoretical review on multiplex influence maximization models: Theories, methods, challenges, and future directions. Expert Systems with Applications 266:125990. <https://doi.org/https://doi.org/10.1016/j.eswa.2024.125990>, URL <https://www.sciencedirect.com/science/article/pii/S0957417424028574>

Ata SK, Fang Y, Wu M, et al (2021) Multi-view collaborative network embedding. ACM Trans Knowl Discov Data 15(3). <https://doi.org/10.1145/3441450>, URL <https://doi.org/10.1145/3441450>

Baptista A, Gonzalez A, Baudot A (2022) Universal multilayer network exploration by random walk with restart. Communications Physics 5(1):170. <https://doi.org/10.1038/s42005-022-00937-9>

Baptista A, Sánchez-García RJ, Baudot A, et al (2023) Zoo guide to network embedding. Journal of Physics: Complexity 4(4):042001. <https://doi.org/10.1088/2632-072X/ad0e23>, URL <https://dx.doi.org/10.1088/2632-072X/ad0e23>

Belkin M, Niyogi P (2001) Laplacian eigenmaps and spectral techniques for embedding and clustering. In: Proceedings of the 15th International Conference on Neural Information Processing Systems: Natural and Synthetic. MIT Press, Cambridge, MA, USA, NIPS'01, p 585–591

Berkhin P (2005) A survey on pagerank computing. *Internet mathematics* 2(1):73–120

Bianconi G (2018) Multilayer Networks: Structure and Function. Oxford University Press

Bielak P, Kajdanowicz T (2024) Representation learning in multiplex graphs: Where and how to fuse information? In: Franco L, de Matalier C, Paszynski M, et al (eds) Computational Science – ICCS 2024. Springer Nature Switzerland, Cham, pp 3–18

Bishop CM, Bishop H (2024) Deep Learning: Foundations and Concepts. Springer

Boccaletti S, Bianconi G, Criado R, et al (2014) The structure and dynamics of multilayer networks. *Physics Reports* 544:1 – 122. URL <https://doi.org/10.1016/j.physrep.2014.07.001>

Chen KJ, Qiu Y, Liu Z, et al (2024) Layer imbalance-aware multiplex network embedding. *Knowledge and Information Systems* 66(6):3547–3569. <https://doi.org/10.1007/s10115-024-02072-z>, URL <https://doi.org/10.1007/s10115-024-02072-z>

Chu X, Fan X, Yao D, et al (2019) Noise-aware network embedding for multiplex network. In: 2019 International Joint Conference on Neural Networks (IJCNN), pp 1–8, <https://doi.org/10.1109/IJCNN.2019.8851949>

Cui P, Wang X, Pei J, et al (2019) A survey on network embedding. *IEEE Transactions on Knowledge and Data Engineering* 31(5):833–852. <https://doi.org/10.1109/TKDE.2018.2849727>

De Domenico M, Solé-Ribalta A, Cozzo E, et al (2013) Mathematical formulation of multilayer networks. *Phys Rev X* 3:041022. <https://doi.org/10.1103/PhysRevX.3.041022>, URL <https://link.aps.org/doi/10.1103/PhysRevX.3.041022>

De Domenico M, Nicosia V, Arenas A, et al (2015) Structural reducibility of multilayer networks. *Nature Communications* 6(1):6864. <https://doi.org/10.1038/ncomms7864>, URL <https://doi.org/10.1038/ncomms7864>

Defferrard M, Bresson X, Vandergheynst P (2016) Convolutional neural networks on graphs with fast localized spectral filtering. In: Lee D, Sugiyama M, Luxburg U, et al (eds) *Advances in Neural Information Processing Systems*, vol 29. Curran Associates, Inc., URL https://proceedings.neurips.cc/paper_files/paper/2016/file/04df4d434d481c5bb723be1b6df1ee65-Paper.pdf

Delvenne JC, Schaub MT, Yaliraki SN, et al (2013) The Stability of a Graph Partition: A Dynamics-Based Framework for Community Detection, Springer New York, New York, NY, pp 221–242. https://doi.org/10.1007/978-1-4614-6729-8_11, URL https://doi.org/10.1007/978-1-4614-6729-8_11

Domenico MD, Lima A, Mougel P, et al (2013) The anatomy of a scientific rumor. *Scientific Reports* 3. <https://doi.org/10.1038/srep02980>

Du X, Yan J, Zhang R, et al (2022) Cross-network skip-gram embedding for joint network alignment and link prediction. *IEEE Transactions on Knowledge and Data Engineering* 34(3):1080–1095. <https://doi.org/10.1109/TKDE.2020.2997861>

El Gheche M, Frossard P (2021) Multilayer graph clustering with optimized node embedding. In: 2021 IEEE Data Science and Learning Workshop (DSLW), pp 1–6, <https://doi.org/10.1109/DSLW51110.2021.9523401>

Estrada E (2011) The Structure of Complex Networks: Theory and Applications. Oxford University Press, <https://doi.org/10.1093/acprof:oso/9780199591756.001.0001>, URL <https://doi.org/10.1093/acprof:oso/9780199591756.001.0001>

Fu D, Xu Z, Li B, et al (2020) A view-adversarial framework for multi-view network embedding. In: Proceedings of the 29th ACM International Conference on Information & Knowledge Management. Association for Computing Machinery, New York, NY, USA, CIKM '20, p 2025–2028, <https://doi.org/10.1145/3340531.3412127>, URL <https://doi.org/10.1145/3340531.3412127>

Gallo L, Latora V, Pulvirenti A (2024) Multiplexsage: A multiplex embedding algorithm for inter-layer link prediction. *IEEE Transactions on Neural Networks and Learning Systems* 35(10):14075–14084. <https://doi.org/10.1109/TNNLS.2023.3274565>

Ghorbani M, Soleymani M, Rabiee H (2018) Multi-layered graph embedding with graph convolution networks. <https://doi.org/10.48550/arXiv.1811.08800>

Grover A, Leskovec J (2016) node2vec: Scalable feature learning for networks. In: Proceedings of the 22nd ACM SIGKDD International Conference on Knowledge Discovery and Data Mining. Association for Computing Machinery, New York, NY, USA, KDD '16, p 855–864, <https://doi.org/10.1145/2939672.2939754>, URL <https://doi.org/10.1145/2939672.2939754>

Gu W, Tandon A, Ahn YY, et al (2021) Principled approach to the selection of the embedding dimension of networks. *Nature Communications* 12(1):3772. <https://doi.org/10.1038/s41467-021-23795-5>, URL <https://doi.org/10.1038/s41467-021-23795-5>

Gutmann M, Hyvärinen A (2010) Noise-contrastive estimation: A new estimation principle for unnormalized statistical models. *Journal of Machine Learning Research - Proceedings Track* 9:297–304

Hajiseyedjavadi S, Lin YR, Pelechrinis K (2019) Learning embeddings for multiplex networks using triplet loss. *Applied Network Science* 4(1):125. <https://doi.org/10.1007/s41109-019-0242-0>, URL <https://doi.org/10.1007/s41109-019-0242-0>

Hamilton WL, Ying R, Leskovec J (2017) Inductive representation learning on large graphs. In: *Proceedings of the 31st International Conference on Neural Information Processing Systems*. Curran Associates Inc., Red Hook, NY, USA, NIPS’17, p 1025–1035

Han B, Wei Y, Wang X, et al (2021) Multiplex graph clustering with network embedding technique: Review, methods and challenges. In: *2021 IEEE International Conference on Unmanned Systems (ICUS)*, pp 596–601, <https://doi.org/10.1109/ICUS52573.2021.9641270>

Hochreiter S, Schmidhuber J (1997) Long short-term memory. *Neural Computation* 9(8):1735–1780. <https://doi.org/10.1162/neco.1997.9.8.1735>

Hou M, Ren J, Zhang D, et al (2020) Network embedding: Taxonomies, frameworks and applications. *Computer Science Review* 38:100296. <https://doi.org/https://doi.org/10.1016/j.cosrev.2020.100296>, URL <https://www.sciencedirect.com/science/article/pii/S1574013720303968>

Huang Z, Li X, Ye Y, et al (2021a) Mr-gcn: multi-relational graph convolutional networks based on generalized tensor product. In: *Proceedings of the Twenty-Ninth International Joint Conference on Artificial Intelligence, IJCAI’20*

Huang Z, Silva A, Singh A (2021b) A broader picture of random-walk based graph embedding. In: Proceedings of the 27th ACM SIGKDD Conference on Knowledge Discovery & Data Mining. Association for Computing Machinery, New York, NY, USA, KDD '21, p 685–695, <https://doi.org/10.1145/3447548.3467300>, URL <https://doi.org/10.1145/3447548.3467300>

Jaccard P (1901) Étude comparative de la distribution florale dans une portion des Alpes et du Jura. Bulletin de la Société Vaudoise des Sciences Naturelles <https://doi.org/10.5169/SEALS-266450>, URL <https://www.e-periodica.ch/digbib/view?pid=bsv-002:1901:37::790>, medium: text/html,application/pdf,text/html Publisher: Imprimerie Corbaz & Comp.

Khan MR, Blumenstock JE (2019) Multi-gcn: graph convolutional networks for multi-view networks, with applications to global poverty. In: Proceedings of the Thirty-Third AAAI Conference on Artificial Intelligence and Thirty-First Innovative Applications of Artificial Intelligence Conference and Ninth AAAI Symposium on Educational Advances in Artificial Intelligence. AAAI Press, AAAI'19 / IAAI'19 / EAAI'19, <https://doi.org/10.1609/aaai.v33i01.3301606>, URL <https://doi.org/10.1609/aaai.v33i01.3301606>

Kipf TN, Welling M (2017) Semi-supervised classification with graph convolutional networks. URL <https://arxiv.org/abs/1609.02907>, arXiv:1609.02907

Kivelä M, Arenas A, Barthelemy M, et al (2014) Multilayer networks. Journal of Complex Networks 2:203–271. <https://doi.org/https://doi.org/10.1093/comnet/cnu016>

Leskovec J, Faloutsos C (2006) Sampling from large graphs. In: Proceedings of the 12th ACM SIGKDD International Conference on Knowledge Discovery and Data Mining. Association for Computing Machinery, New York, NY, USA, KDD '06, p

631–636, <https://doi.org/10.1145/1150402.1150479>, URL <https://doi.org/10.1145/1150402.1150479>

Li AQ, Ahmed A, Ravi S, et al (2014) Reducing the sampling complexity of topic models. In: Proceedings of the 20th ACM SIGKDD International Conference on Knowledge Discovery and Data Mining. Association for Computing Machinery, New York, NY, USA, KDD '14, p 891–900, <https://doi.org/10.1145/2623330.2623756>, URL <https://doi.org/10.1145/2623330.2623756>

Li J, Chen C, Tong H, et al (2018) Multi-Layered Network Embedding, SIAM, pp 684–692. <https://doi.org/10.1137/1.9781611975321.77>, URL <https://pubs.siam.org/doi/abs/10.1137/1.9781611975321.77> <https://pubs.siam.org/doi/pdf/10.1137/1.9781611975321.77>

Lichtenwalter R, Chawla NV (2012) Link prediction: Fair and effective evaluation. In: 2012 IEEE/ACM International Conference on Advances in Social Networks Analysis and Mining, pp 376–383, <https://doi.org/10.1109/ASONAM.2012.68>

Liu W, Chen Py, Yeung S, et al (2017) Principled multilayer network embedding. In: 2017 IEEE International Conference on Data Mining Workshops (ICDMW), pp 134–141, <https://doi.org/10.1109/ICDMW.2017.23>

Luo D, Bian Y, Yan Y, et al (2023) Random walk on multiple networks. IEEE Transactions on Knowledge and Data Engineering 35(8):8417–8430. <https://doi.org/10.1109/TKDE.2022.3221668>

László L, Lov L, Erdos O (1996) Random walks on graphs: A survey. Combinatorics, Paul Erdos is Eighty 2:1–46

Ma Y, Wang S, Aggarwal CC, et al (2019) Multi-dimensional graph convolutional networks. In: Proceedings of the 2019 siam international conference on data mining,

SIAM, pp 657–665

Matsuno R, Murata T (2018) Mell: Effective embedding method for multiplex networks. In: Companion Proceedings of the The Web Conference 2018. International World Wide Web Conferences Steering Committee, Republic and Canton of Geneva, CHE, WWW '18, p 1261–1268, <https://doi.org/10.1145/3184558.3191565>, URL <https://doi.org/10.1145/3184558.3191565>

Menand N, Seshadhri C (2024) Link prediction using low-dimensional node embeddings: The measurement problem. Proceedings of the National Academy of Sciences 121(8):e2312527121. <https://doi.org/10.1073/pnas.2312527121>, URL <https://www.pnas.org/doi/abs/10.1073/pnas.2312527121>, <https://www.pnas.org/doi/pdf/10.1073/pnas.2312527121>

Mescheder L, Geiger A, Nowozin S (2018) Which training methods for gans do actually converge? In: International Conference on Machine learning (ICML)

Mikolov T, Chen K, Corrado GS, et al (2013a) Efficient estimation of word representations in vector space. In: International Conference on Learning Representations, URL <https://api.semanticscholar.org/CorpusID:5959482>

Mikolov T, Sutskever I, Chen K, et al (2013b) Distributed representations of words and phrases and their compositionality. In: Neural Information Processing Systems, URL <https://api.semanticscholar.org/CorpusID:16447573>

Nguyen HT, Dinh TN, Vu T (2015) Community detection in multiplex social networks. In: 2015 IEEE Conference on Computer Communications Workshops (INFOCOM WKSHPS), pp 654–659, <https://doi.org/10.1109/INFCOMW.2015.7179460>

Ning N, Wu B, Peng C (2018) Representation learning based on influence of node for multiplex network. In: 2018 IEEE Third International Conference on Data Science

in Cyberspace (DSC), pp 865–872, <https://doi.org/10.1109/DSC.2018.00139>

Ning N, Long F, Wang C, et al (2020) Nonlinear structural fusion for multiplex network. *Complex* 2020. <https://doi.org/10.1155/2020/7041564>, URL <https://doi.org/10.1155/2020/7041564>

Ning N, Li Q, Zhao K, et al (2021a) Multiplex network embedding model with high-order node dependence. *Complexity* 2021(1):6644111. <https://doi.org/https://doi.org/10.1155/2021/6644111>, URL <https://onlinelibrary.wiley.com/doi/abs/10.1155/2021/6644111>, <https://onlinelibrary.wiley.com/doi/pdf/10.1155/2021/6644111>

Ning N, Yang Y, Song C, et al (2021b) An adaptive node embedding framework for multiplex networks. *Intell Data Anal* 25(2):483–503. <https://doi.org/10.3233/IDA-195065>, URL <https://doi.org/10.3233/IDA-195065>

Page L, Brin S, Motwani R, et al (1999) The pagerank citation ranking : Bringing order to the web. In: The Web Conference, URL <https://api.semanticscholar.org/CorpusID:1508503>

Park C, Kim D, Han J, et al (2020) Unsupervised attributed multiplex network embedding. *Proceedings of the AAAI Conference on Artificial Intelligence* 34(04):5371–5378. <https://doi.org/10.1609/aaai.v34i04.5985>, URL <https://ojs.aaai.org/index.php/AAAI/article/view/5985>

Perozzi B, Al-Rfou R, Skiena S (2014) Deepwalk: online learning of social representations. In: *Proceedings of the 20th ACM SIGKDD International Conference on Knowledge Discovery and Data Mining*. Association for Computing Machinery, New York, NY, USA, KDD '14, p 701–710, <https://doi.org/10.1145/2623330.2623732>, URL <https://doi.org/10.1145/2623330.2623732>

Pio-Lopez L, Valdeolivas A, Tichit L, et al (2021) MultiVERSE: a multiplex and multiplex-heterogeneous network embedding approach. *Scientific Reports* 11(1):8794. <https://doi.org/10.1038/s41598-021-87987-1>, URL <https://doi.org/10.1038/s41598-021-87987-1>

Qiu J, Dong Y, Ma H, et al (2018) Network embedding as matrix factorization: Unifying deepwalk, line, pte, and node2vec. In: *Proceedings of the Eleventh ACM International Conference on Web Search and Data Mining*. Association for Computing Machinery, New York, NY, USA, WSDM '18, p 459–467, <https://doi.org/10.1145/3159652.3159706>, URL <https://doi.org/10.1145/3159652.3159706>

Qu M, Tang J, Shang J, et al (2017) An attention-based collaboration framework for multi-view network representation learning. In: *Proceedings of the 2017 ACM on Conference on Information and Knowledge Management*. Association for Computing Machinery, New York, NY, USA, CIKM '17, p 1767–1776, <https://doi.org/10.1145/3132847.3133021>, URL <https://doi.org/10.1145/3132847.3133021>

Rainio O, Teuho J, Klén R (2024) Evaluation metrics and statistical tests for machine learning. *Scientific Reports* 14(1):6086. <https://doi.org/10.1038/s41598-024-56706-x>, URL <https://doi.org/10.1038/s41598-024-56706-x>

Ren G, Ding X, Xu XK, et al (2024) Link prediction in multilayer networks via cross-network embedding. *Proceedings of the AAAI Conference on Artificial Intelligence* 38:8939–8947. <https://doi.org/10.1609/aaai.v38i8.28742>, URL <https://ojs.aaai.org/index.php/AAAI/article/view/28742>

Ribeiro LF, Saverese PH, Figueiredo DR (2017) struc2vec: Learning node representations from structural identity. In: *Proceedings of the 23rd ACM SIGKDD International Conference on Knowledge Discovery and Data Mining*. Association for Computing Machinery, New York, NY, USA, KDD '17, p 385–394, <https://doi.org/10.1145/3055399.3055880>, URL <https://doi.org/10.1145/3055399.3055880>

org/10.1145/3097983.3098061, URL <https://doi.org/10.1145/3097983.3098061>

Sánchez-García RJ, Cozzo E, Moreno Y (2014) Dimensionality reduction and spectral properties of multilayer networks. *Phys Rev E* 89:052815. <https://doi.org/10.1103/PhysRevE.89.052815>, URL <https://link.aps.org/doi/10.1103/PhysRevE.89.052815>

Sharma S, Singh A (2016) An efficient method for link prediction in weighted multiplex networks. *Computational Social Networks* 3(1):7. <https://doi.org/10.1186/s40649-016-0034-y>, URL <https://doi.org/10.1186/s40649-016-0034-y>

Shi Y, Han F, He X, et al (2018) mvn2vec: Preservation and collaboration in multi-view network embedding. *ArXiv* abs/1801.06597

Song H, Thiagarajan JJ (2019) Improved deep embeddings for inferencing with multi-layered graphs. In: 2019 IEEE International Conference on Big Data (Big Data), pp 5394–5400, <https://doi.org/10.1109/BigData47090.2019.9005501>

Steck H, Ekanadham C, Kallus N (2024) Is cosine-similarity of embeddings really about similarity? In: Companion Proceedings of the ACM Web Conference 2024. ACM, WWW '24, p 887–890, <https://doi.org/10.1145/3589335.3651526>, URL <http://dx.doi.org/10.1145/3589335.3651526>

Sun Y, Wang S, Hsieh TY, et al (2019) Megan: A generative adversarial network for multi-view network embedding. *ArXiv* abs/1909.01084

Tang J, Qu M, Wang M, et al (2015) Line: Large-scale information network embedding. In: Proceedings of the 24th International Conference on World Wide Web. International World Wide Web Conferences Steering Committee, Republic and Canton of Geneva, CHE, WWW '15, p 1067–1077, <https://doi.org/10.1145/2736277.2741093>, URL <https://doi.org/10.1145/2736277.2741093>

Tsitsulin A, Mottin D, Karras P, et al (2018) Verse: Versatile graph embeddings from similarity measures. In: Proceedings of the 2018 World Wide Web Conference. International World Wide Web Conferences Steering Committee, Republic and Canton of Geneva, CHE, WWW '18, p 539–548, <https://doi.org/10.1145/3178876.3186120>, URL <https://doi.org/10.1145/3178876.3186120>

Veličković P, Cucurull G, Casanova A, et al (2018a) Graph attention networks. URL <https://arxiv.org/abs/1710.10903>, arXiv:1710.10903

Veličković P, Fedus W, Hamilton WL, et al (2018b) Deep graph infomax. URL <https://arxiv.org/abs/1809.10341>, arXiv:1809.10341

Vickers M, Chan S (1981) Representing Classroom Social Structure. Melbourne: Victoria Institute of Secondary Education.

Wang H, Wang J, Wang J, et al (2017) Graphgan: Graph representation learning with generative adversarial nets. ArXiv abs/1711.08267. URL <https://api.semanticscholar.org/CorpusID:19140125>

Wang Q, Jiang H, Jiang Y, et al (2023) Multiplex network infomax: Multiplex network embedding via information fusion. Digital Communications and Networks 9(5):1157–1168. <https://doi.org/https://doi.org/10.1016/j.dcan.2022.10.002>, URL <https://www.sciencedirect.com/science/article/pii/S2352864822002115>

Ward IR, Joyner J, Lickfold C, et al (2022) A practical tutorial on graph neural networks. ACM Comput Surv 54(10s). <https://doi.org/10.1145/3503043>, URL <https://doi.org/10.1145/3503043>

Wilson JD, Baybay M, Sankar R, et al (2021) Analysis of population functional connectivity data via multilayer network embeddings. Network Science 9(1):99–122. <https://doi.org/10.1017/nws.2020.39>

Xie Y, Zhang Y, Gong M, et al (2020) Mgat: Multi-view graph attention networks. *Neural Networks* 132:180–189. <https://doi.org/https://doi.org/10.1016/j.neunet.2020.08.021>, URL <https://www.sciencedirect.com/science/article/pii/S0893608020303105>

Xu L, Wei X, Cao J, et al (2018) Multi-task network embedding. *International Journal of Data Science and Analytics* 8:183 – 198

Yang K, Li J, Liu M, et al (2023) Complex systems and network science: a survey. *Journal of Systems Engineering and Electronics* 34(3):543–573. <https://doi.org/10.23919/JSEE.2023.000080>

Yao K, Liang J, Liang J, et al (2022) Multi-view graph convolutional networks with attention mechanism. *Artificial Intelligence* 307:103708. <https://doi.org/https://doi.org/10.1016/j.artint.2022.103708>, URL <https://www.sciencedirect.com/science/article/pii/S0004370222000480>

You K (2025) Semantics at an angle: When cosine similarity works until it doesn't. URL <https://arxiv.org/abs/2504.16318>, arXiv:2504.16318

Zhang D, Yin J, Zhu X, et al (2020) Network representation learning: A survey. *IEEE Transactions on Big Data* 6(1):3–28. <https://doi.org/10.1109/TB DATA.2018.2850013>

Zhang H, Kou G (2022) Role-based multiplex network embedding. In: Chaudhuri K, Jegelka S, Song L, et al (eds) *Proceedings of the 39th International Conference on Machine Learning, Proceedings of Machine Learning Research*, vol 162. PMLR, pp 26265–26280, URL <https://proceedings.mlr.press/v162/zhang22m.html>

Zhang H, Qiu L, Yi L, et al (2018) Scalable multiplex network embedding. In: *Proceedings of the 27th International Joint Conference on Artificial Intelligence*. AAAI

Press, IJCAI'18, p 3082–3088

Zhou J, Cui G, Hu S, et al (2020) Graph neural networks: A review of methods and applications. *AI Open* 1:57–81. <https://doi.org/https://doi.org/10.1016/j.aiopen.2021.01.001>, URL <https://www.sciencedirect.com/science/article/pii/S2666651021000012>

Zhou K, Ethayarajh K, Card D, et al (2022) Problems with cosine as a measure of embedding similarity for high frequency words. In: Muresan S, Nakov P, Villavicencio A (eds) *Proceedings of the 60th Annual Meeting of the Association for Computational Linguistics (Volume 2: Short Papers)*. Association for Computational Linguistics, Dublin, Ireland, pp 401–423, <https://doi.org/10.18653/v1/2022.acl-short.45>, URL <https://aclanthology.org/2022.acl-short.45/>

Zitnik M, Leskovec J (2017) Predicting multicellular function through multi-layer tissue networks. *Bioinformatics* 33:i190 – i198